https://doi.org/10.5194/egusphere-2023-427
Preprint. Discussion started: 13 March 2023

Impact of chlorine ion chemistry on ozone loss in the middle atmosphere during very large solar proton events

Monali Borthakur[1], Miriam Sinnhuber[1], Alexandra Laeng[1], Thomas Reddmann[1], Peter Braesicke[1], Gabriele Stiller[1], Thomas von Clarmann[1], Bernd Funke[2], Ilya Usoskin[3], Jan Maik Wissing[4], and Olesya Yakovchuk[4]

[1]Institute of Meteorology and Climate research, Karlsruhe Institute of Technology, Karlsruhe, Germany
[2]Instituto de Astrofísica de Andalucía, CSIC, Granada, Spain
[3]University of Oulu, Oulu, Finland
[4]University of Rostock, Rostock, Germany

Correspondence: Monali Borthakur (monali.borthakur@kit.edu)

Abstract.

Solar coronal mass ejections can accelerate charged particles, mostly protons, to high energies, causing Solar Particle Events (SPEs). Such energetic particles can precipitate upon the Earth's atmosphere, mostly in polar regions because of the geomagnetic shielding. Here, SPE induced chlorine activation due to ion-chemistry can occur and the activated chlorine depletes ozone in the polar middle atmosphere. We use a state of the art 1D stacked-box model called Exoplanetary Terrestrial Ion Chemistry (ExoTIC), of atmospheric ion and neutral composition to investigate such events in the Northern Hemisphere (NH). Measurement data from the Michelson Interferometer for Passive Atmospheric Sounding (MIPAS) on ENVISAT were used to evaluate the model results using the Halloween SPE in late October 2003, a well-known large event, as a test field. Sensitivity tests were carried out for different model settings with a focus on the chlorine species of HOCl and $ClONO_2$ as well as O_3 and NO_y. The model studies were carried out in the northern hemisphere for a high latitude of 67.5° N, inside the polar cap. Comparison of the simulated effects against MIPAS observations for the Halloween SPE revealed a rather good temporal and spatial agreement for HOCl, ozone and NO_y. For $ClONO_2$, a good spatial agreement was found. The best model setting was the one with full ion-chemistry where O(^{1}D) was set to photo-chemical equilibrium. HOCl and ozone changes are very well reproduced by the model, specially for night-time. HOCl was found to be the main active chlorine species under night-time conditions resulting in an increase of more than 0.2 ppbv. Further, $ClONO_2$ enhancements of 0.2-0.3 ppbv have been observed both during daytime and night-time. In a nutshell, the most appropriate model setting delivers satisfying result, i.e. the model can be considered to be positively validated. Model settings that compared best with MIPAS observations were applied to an extreme solar event in 775 A.D., presumably a once in a 1000 year event. With the model applied to this scenario, assessment can be made what is to be expected at worst for effects of a SPE on the middle atmosphere. Here, a systematic analysis comparing the impact of the Halloween SPE and the extreme event on the Earth's middle atmosphere is presented. As seen from the model simulations, both events were able to perturb the polar stratosphere and mesosphere, with a high production of NO_y and HO_x. Longer lasting and stronger stratospheric ozone loss was also seen for the extreme event. Qualitative difference between the two events and a long lasting impact on HOCl and HCl for the extreme event was found. Chlorine ion-chemistry

https://doi.org/10.5194/egusphere-2023-427
Preprint. Discussion started: 13 March 2023

contributed to a stratospheric ozone loss of 2.4 % during daytime and 10 % during night-time during the Halloween SPE as seen with time dependent ionisation rates applied to the model. Furthermore, while comparing the two events just for the event day, an ozone loss of 10 % and 20 % was found during the Halloween SPE and the extreme event respectively which was due to the impact of chlorine ion-chemistry.

1 Introduction

High energetic particles (e.g. electrons and protons) that precipitate at high latitudes can alter the chemical composition of the atmosphere by different photo-chemical reactions. Such reactions ordered by increasing energy are, for example, excitation, photo-dissociation, photo-ionisation and dissociative ionisation. These particles can come from various sources in outer space, accelerated by different processes to different energies. They affect different altitude ranges of the atmosphere. Such sources are, for example, galactic cosmic rays (GCRs), with protons and nuclei of energies ranging from hundreds of MeV to GeV; coronal mass ejections and solar particle events with protons of energies from MeV to GeV that precipitate into the earth's atmosphere during solar proton events; auroral electrons during substorms accelerated to energies from 10 keV to hundreds of keV; and medium and high energy electrons in the radiation belts to energies from tens of keV into the MeV range. This mainly happens due to primary collision processes and subsequent ion and neutral chemistry reactions. This study involves solar particle events (SPEs) which can also induce geomagnetic disturbances in the earth's magnetosphere leading to energetic electron precipitation (EEP) events. Recent studies of energetic particle precipitation events (EPP) found significant co-variability in mesospheric ozone. This finding highlighted the need to improve ion chemistry modeling in the D-region for altitudes below 90 km in the ionosphere (Funke et al., 2011) to capture the EPP ozone interaction. HNO_3 increases measured during solar proton events (SPE) cannot be reproduced using the standard parameterization of HO_x and NO_x production, while models considering D-region ion-chemistry in detail agree with the observations (Verronen et al., 2016). The HO_x and NO_x parameterization cannot reproduce the longer-term effects of ion-chemistry on for example, reactive nitrogen partitioning, ozone, and dynamics of the middle atmosphere (Kvissel et al., 2012).

In the case of parameterized NO_x, NO is produced when $N(^2D)$ reacts with molecular oxygen, shown in Reaction R1 (Porter et al., 1976; Jackman et al., 2005). This reaction is a major source of NO in the stratosphere, mesosphere and lower thermosphere (Rusch et al., 1981; Barth, 1992).

$$N(^2D) + O_2 \longrightarrow NO + O \tag{R1}$$

O_2 can also react with the ground state $N(^4S)$, that is temperature dependent and is a major source of NO in the thermosphere above $\sim$ 120 km (Sinnhuber et al., 2012; Barth, 1992). NO can be destroyed by Reaction R2, which is an effective loss mechanism for NO_x, also known as the scavenging reaction (Jackman et al., 2005):

$$N(^4S) + NO \longrightarrow N_2 + O \tag{R2}$$

The excited states of N form NO, while ground state can destroy NO which is relevant in the stratosphere, mesosphere and lower thermosphere. The partitioning between the ground and the excited states determine the amount of NO_x formed

https://doi.org/10.5194/egusphere-2023-427
Preprint. Discussion started: 13 March 2023

(Sinnhuber et al., 2012; Nieder et al., 2014) thereby making Reaction R2 the driver of parameterised NO_x. Thus, Reaction R2 makes the difference between full ion-chemistry and parameterised NO_x formation. The main processes responsible for the odd hydrogen (HO_x= H,OH,HO_2) formation during energetic particle precipitation events, were considered by Solomon et al. (1981). They take place after the initial formation of ion pairs. Solomon et al. (1981) considered the ion-chemistry processes leading to a release of HO_x during energetic particle precipitation events. They found that the main process responsible is the uptake of water vapour into large cluster ions and the subsequent release of H during recombination reactions of these cluster ions. Large cluster ions can then be formed by reaction pathways like (Sinnhuber et al., 2012):

$$O_2^+(H_2O) + H_2O \longrightarrow H_3O^+(OH) + O_2 \tag{R3}$$

$$O_2^+(H_2O) + H_2O \longrightarrow H^+(H_2O) + OH + O_2 \tag{R4}$$

These protonised water cluster ions can then recombine with electrons to form H and OH.

$$H_3O^+(OH) + e^- \longrightarrow H_2O + H + OH \tag{R5}$$

During SPEs, highly energetic solar protons and the secondary electrons also ionize neutral species and produce hydrogen and nitrogen radicals leading to ozone destruction through catalytic cycles in the stratosphere and mesosphere. Different studies found ozone depletion in the mesosphere during SPEs, for example, Weeks et al. (1972) who studied a large polar cap absorption event in 1969 that was explained as a result of the formation of odd hydrogen (Swider and Keneshea, 1973). The chlorine catalytic cycles of ozone destruction are also very efficient around 40 km (Lary, 1997). SPE induced changes of chlorine species can contribute to the short-term ozone depletion occurring after the SPE (von Clarmann et al., 2005). This influence is indirect and is mainly caused by NO_x and HO_x enhancements. The hypochlorous acid (HOCl) catalytic cycle acts as a link between chlorine and HO_x enhancements as a result of the SPEs, which then speeds up the following three reaction sequence involving Reactions R6, R7 and R8:

$$OH + HCl \longrightarrow H_2O + Cl \tag{R6}$$

$$Cl + O_3 \longrightarrow ClO + O_2 \tag{R7}$$

$$ClO + HO_2 \longrightarrow HOCl + O_2 \tag{R8}$$

von Clarmann et al. (2005) showed an enhancement of chlorine monoxide, ClO and HOCl immediately after the SPE. They concluded that this was due to the Reactions R7 and R8. During an SPE, HOCl and reactive Cl present in the stratosphere can react with OH and HO_2 respectively, to form ClO. Other reactions of Cl with HO_2 and H_2O_2 can yield in the production of HCl, which is the most important stratospheric reservoir species of Cl. The Reactions R9, R10, R11 and R12 are relevant to the study in Sect. 4.

$$HOCl + OH \longrightarrow ClO + H_2O \tag{R9}$$

https://doi.org/10.5194/egusphere-2023-427
Preprint. Discussion started: 13 March 2023

$$Cl + HO_2 \longrightarrow ClO + OH \quad \text{(R10)}$$

$$Cl + HO_2 \longrightarrow HCl + O_2 \quad \text{(R11)}$$

$$Cl + H_2O_2 \longrightarrow HCl + HO_2 \quad \text{(R12)}$$

SPE induced NO_x enhancements is essential regarding production of $ClONO_2$. López-Puertas et al. (2005) and von Clarmann et al. (2005) reported the first experimental confirmation of Reaction R13 under SPE conditions.

$$ClO + NO_2 + M \longrightarrow ClONO_2 + M \quad \text{(R13)}$$

During SPEs, NO_x, HO_x and chlorine catalytic cycles are responsible for ozone loss in the middle atmosphere at different altitudes.

1.1 Hydrogen catalytic cycles

Catalytic cycles involving HO_2 are very important in the lower stratosphere (10-30 km). The fastest of these cycles is shown in Reactions R14, R15 and R16.

$$OH + O_3 \longrightarrow HO_2 + O_2 \quad \text{(R14)}$$

$$HO_2 + O \longrightarrow OH + O_2 \quad \text{(R15)}$$

$$\text{Net} : O_3 + O \longrightarrow O_2 + O_2 \quad \text{(R16)}$$

Another example of HO_x catalytic destruction cycles that is important in the middle and upper mesosphere (above 60 km), is shown in Reactions R17 and R18 (Bates and Nicolet, 1950). In every chain of Reactions R17 and R18, one molecule of O_3, $O(^3P)$ or $O(^1D)$ is lost while reforming H and OH and thereby producing a net ozone loss (Reaction R19).

$$H + O_3 \longrightarrow OH + O_2 \quad \text{(R17)}$$

$$OH + O \longrightarrow H + O_2 \quad \text{(R18)}$$

$$\text{Net} : O_3 + O \longrightarrow O_2 + O_2 \quad \text{(R19)}$$

1.2 Nitrogen catalytic cycle

In the lower stratosphere, ozone loss is mainly due to the catalytic cycle with NO_x governed by the reactions R20 and R21 in which case the loss of ozone is more persistent due to the longer lifetimes of NO_x.

$$NO + O_3 \longrightarrow NO_2 + O_2 \quad \text{(R20)}$$

$$NO_2 + O \longrightarrow NO + O_2 \quad \text{(R21)}$$

$$\text{Net} : O_3 + O \longrightarrow O_2 + O_2 \quad \text{(R22)}$$

https://doi.org/10.5194/egusphere-2023-427
Preprint. Discussion started: 13 March 2023

1.3 Chlorine catalytic cycles

The focus of this paper is the impact of charged chlorine species during a SPE. Negative chlorine species constitute a significant part of the total anions in the mesosphere (Chakrabarty and Ganguly, 1989; Fritzenwallner and Kopp, 1998). The chlorine negative ion is the most important ion of the lower D region during day and night time. Other D region negative ions like O_2^-, O^-, CO_3^-, OH^-, NO_2^- and NO_3^- can react with HCl to produce Cl^- which forms $Cl^-(X)$, where X = (HCl, H_2O, CO_2 and HO_2) (Kopp and Fritzenwallner, 1997). $Cl^-$and $Cl^-(H_2O)$ are the most abundant chlorine ions in the mesosphere. Both species can react with atomic hydrogen re-releasing HCl and some of the recombination reactions of negative chlorine species with positive ions like H^+ release Cl, ClO, $ClNO_2$, and Cl_2. Since the ion reactions are faster, the SPE impacts due to chlorine ion-chemistry are expected to occur without any notable delay. The reactions involving charged and uncharged chlorine species along with the reaction rate coefficients are given in Table A1.

Apart from the NO_x and HO_x catalytic cycles, solar proton events can also affect stratospheric chlorine chemistry, but whether solar protons effectively activate or deactivate chlorine depends on illumination conditions. The ion production rates increases during a SPE and influences the chemistry of both charged and uncharged chlorine species. The neutral compounds of chlorine can then contribute to ozone loss. The ClO_x ozone loss catalytic cycle:

$$ClO + O \longrightarrow Cl + O_2 \quad \text{(R23)}$$

$$Cl + O_3 \longrightarrow ClO + O_2 \quad \text{(R24)}$$

$$\text{Net} : O_3 + O \longrightarrow O_2 + O_2 \quad \text{(R25)}$$

is the main cycle responsible for ozone loss in the middle and upper stratosphere between 40 and 50 km (Daniel et al., 1999). Other uncharged chlorine cycles, for example, ClO_x cycle where two molecules of chlorine monoxide react with each other (Reactions R26, R27, R28, R29 and R30) is mainly effective between 20 and 30 km (Lary, 1997). As suggested by J. C. Farman and Shanklin. (1985), the cycle of chlorine monoxide reacting with nitric oxide (Reactions R31, R32, R33 and R34) is most important in the 15 to 50 km altitude range.

$$ClO + ClO \longrightarrow Cl_2O_2 \quad \text{(R26)}$$

$$Cl_2O_2 + h\nu \longrightarrow Cl + ClO_2 \quad \text{(R27)}$$

$$ClO_2 \longrightarrow Cl + O_2 \quad \text{(R28)}$$

$$2 * (Cl + O_3 \longrightarrow ClO + O_2) \quad \text{(R29)}$$

$$\text{Net} : 2O_3 \longrightarrow 3O_2 \quad \text{(R30)}$$

$$ClO + NO \longrightarrow Cl + NO_2 \quad \text{(R31)}$$

$$NO_2 + O(^3P) \longrightarrow NO + O_2 \quad \text{(R32)}$$

$$Cl + O_3 \longrightarrow ClO + O_2 \quad \text{(R33)}$$

$$\text{Net} : O(^3P) + O_3 \longrightarrow 2O_2 \quad \text{(R34)}$$

https://doi.org/10.5194/egusphere-2023-427
Preprint. Discussion started: 13 March 2023

However, ClO can also react with nitrogen dioxide, NO_2 which is most efficient in the lower stratosphere (Reactions R35, R36, R37, R38 and R39), and is another effective ozone loss cycle between 15 and 40 km (Lary, 1997).

$$ClO + NO_2 \longrightarrow ClONO_2 \quad \text{(R35)}$$

$$ClONO_2 + h\nu \longrightarrow Cl + NO_3 \quad \text{(R36)}$$

$$NO_3 + h\nu \longrightarrow NO + O_2 \quad \text{(R37)}$$

$$Cl + O_3 \longrightarrow ClO + O_2 \quad \text{(R38)}$$

$$\text{Net} : O(^3P) + O_3 \longrightarrow 2O_2 \quad \text{(R39)}$$

The present paper deals with changes of HOCl, $ClONO_2$, ozone and NO_y occurring in the Northern Hemisphere at a high latitude of 67.5 °N during the Halloween SPE from mid October to early November 2003, peaking around October 28-29. The Halloween SPE was one of the largest SPEs in the satellite era and consisted of a series of solar flares and coronal mass ejections. Such large events mainly occur in the declining phase of the solar maximum. Changes in the composition of HOCl, $ClONO_2$, ozone and NO_y species during the Halloween SPE have been previously reported in Funke et al. (2011) and Jackman et al. (2008). Funke et al. (2011) used different models to investigate the SPE induced changes and Jackman et al. (2008) used version 3 of the Whole Atmosphere Community Climate Model (WACCM). Both studies compared with the MIPAS observations from polar orbit satellite ENVISAT. Damiani et al. (2012) also looked at chlorine species (i.e., HOCl, $ClONO_2$, ClO and HCl) using MLS and MIPAS data and version 4 of the WACCM model during SPEs of 17 and 20 January 2005. However they did not consider the D region ion-chemistry. Here, we studied the temporal evolution of changes of the respective chemical constituents considering the D region ion-chemistry in a 1D stacked box model, Exoplanetary Terrestrial Ion Chemistry (ExoTIC). The ion-chemistry was implemented by Winkler et al. (2009) upon which ExoTIC is based, but we compare with the MIPAS observations, which provide a better picture of the polar cap region compared to Winkler et al. (2009) who compared HALOE HCl observations that were less densely sampled than MIPAS data.

In order to have a better comparison of ExoTIC simulations with MIPAS observations, we ensured that they are sampled inside the polar vortex. The polar vortex is a large circumpolar cyclone which dominates the circulation in the polar winter stratosphere which forms due to decreased solar insolation (Harvey et al., 2015). The assumption is that the air inside the polar vortex is horizontally well mixed and separated from air masses outside the vortex. That allows us to simulate it in a 1D vertical model. The ionisation during particle precipitation in the polar cap is also assumed to be inside the polar vortex where NO_x is conserved which makes it better comparable to the 1D model. The procedure is described in detail in the Sect. 3.1.

The Halloween SPE is later compared with an exceptionally strong cosmic ray event that occurred in 774/775 A.D. It was derived from the historical records in radiocarbon ^{14}C measured in tree ring archives and later confirmed by ^{10}Be and ^{36}Cl cosmogenic nuclides. Although various scenarios were initially proposed, it is concluded now that the event was caused by solar energetic particles (Sukhodolov et al., 2017). ^{10}Be and ^{14}C implied that the event had a very hard spectrum and thereby very high energetic protons. It is the greatest solar energetic particle storm known for the last 11 millennia (the Holocene), serving as a likely worst-case scenario being 40–50 times stronger than the largest directly observed event on 23rd February

https://doi.org/10.5194/egusphere-2023-427
Preprint. Discussion started: 13 March 2023

1956 (Usoskin et al., 2013). This event was transient, as estimated using the ratio of different cosmogenic isotopes (Mekhaldi et al., 2015).

This paper is organised as follows. Section 2 describes the ionisation rates, model framework, simulations and the satellite observations used to evaluate the model. Section 3 presents the results of the model evaluation with MIPAS satellite observations. An overview of the changes in chlorine species, ozone and NO_y induced by the SPE is presented. Section 4 presents a case study comparing model simulations of the Halloween SPE with the extreme solar event. Section 5 shows some results describing the impact of chlorine ion-chemistry on ozone loss. In sect. 6, a conclusion is provided to check if the data is well understood, a summary of how our results compare to previous studies. Finally an assessment is given how further studies could improve our current knowledge on SPE induced ozone loss due to chlorine ion-chemistry.

2 Data and methods

2.1 Ionisation rates

The ionisation rates (IRs) used for the Halloween SPE were obtained from the Atmospheric Ionization during Substorm (AISstorm) model which is an enhanced version of the Atmospheric Ionization Module Osnabrück (AIMOS) model (Wissing and Kallenrode, 2009). The AIMOS model computes ionization rates by precipitating electrons, protons and alpha particles for the whole atmosphere based on particle flux measurements from Polar Operational Environmental Satellites (POES), the Meteorological Operational satellites (Metop) and the Geostationary Operational Environmental Satellites (GOES). The treatment of the electron fluxes is in the energy range (0.154–300 keV), protons have an energy range of 0.154 eV to 500 MeV. In the AIMOS v2.0-AISstorm model, both the time resolution (0.5 hr) and spatial resolution has been improved compared to AIMOS. For a comparison of the model results with MIPAS observations, the time dependent ionisation rates were put into ExoTIC. Figure 1 on the left side shows the temporal evolution of ion pair production rates for protons, electrons and alpha particles varying over the time period, 25$^{\text{th}}$ October to 4$^{\text{th}}$ November 2003 from the AISstorm model. These IRs are averaged over the longitudes for the latitude of 67.5 °N, in the polar cap region and are also daily averaged. For the extreme event, integrated ionisation rates were taken from an extreme SPE of 23 February 1956 (SPE 56) (Meyer et al., 1956), which was the strongest observed event with ground-level enhancement (GLE) > 4000 %. These integrated IRs were scaled by a factor of 70 (Usoskin and Kovaltsov, 2012) in order to represent a one in a 1000 year event. The factor 70 was a rough estimate to scale the fluxes of particles and excess radiation such that the energy spectrum of SPE 56 was comparable to the isotope signals of the extreme event. Figure 1 on the right shows the ionisation rate profiles for both the events. The profiles for the Halloween SPE show average IRs for October 27 (day 301) and October 28 (day 302) before the SPE (in blue) and the average IRs for October 28 and October 29 during the main SPE phase (in green). It can be observed that the ionisation rates for the stratosphere and lower mesosphere in case of the extreme event is about 1-2 orders of magnitude higher compared to the Halloween SPE main phase. This is because the extreme event contained protons of energies up to a few GeV, compared to about only a few MeV protons for the Halloween SPE, the ionisation rates for the same can be seen to reach much further down to the surface.

https://doi.org/10.5194/egusphere-2023-427
Preprint. Discussion started: 13 March 2023

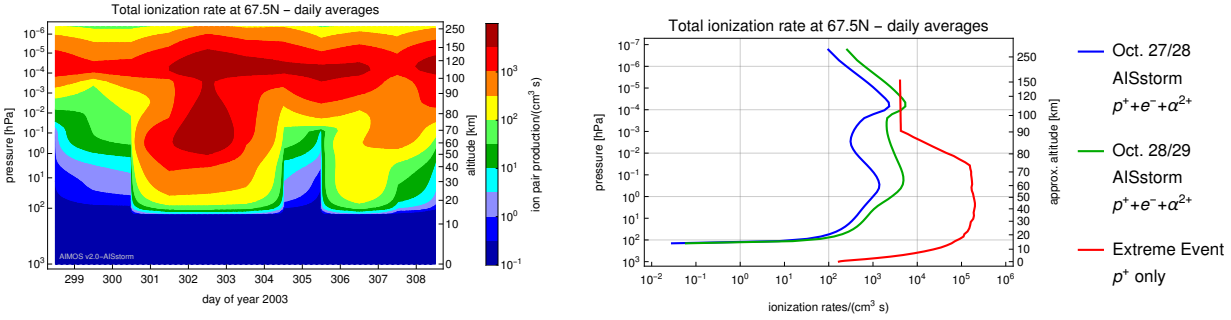

Figure 1. Time dependent and daily averaged ionisation rates (IRs) from 25^{th} October to 4^{th} November 2003 obtained from the AISstorm model for the latitude of 67.5 °N (left); Mean ionisation rates (IRs) before the SPE (Oct 27-28), and in SPE main phase (Oct 28-29) obtained from AISstorm and mean IRs of the extreme event for the same latitude of 67.5° N (right).

2.2 Description of the 1D model and Experiments

The Exoplanetary Terrestrial Ion Chemistry model ExoTIC is a 1-dimensional stacked-box model of the atmospheric neutral and ion composition (Herbst et al., 2022). The ion-chemistry is based on the UBIC (University of Bremen ion-chemistry) model developed by Winkler et al. (2009) for the terrestrial middle atmosphere. The neutral chemistry is based on the SLIMCAT model by Chipperfield (1999). It accounts for photo-ionisation of NO by Lyman-α radiation, photo-dissociation of charged species and photo-detachment of electrons but doesn't contain any diffusion or horizontal and vertical transport. It first simulates a neutral atmosphere and contains the time evolution of 106 charged and 58 neutral species, which interact due to neutral, neutral–ion, and ion–ion gas-phase reactions, as well as photolysis and photoelectron attachment and detachment reactions (Sinnhuber et al., 2012). The model contains boxes of 2.7 km each in height, which is the same as the background atmosphere that is used as input. For the studies performed here, the background atmosphere was taken from the EMAC (ECHAM/MESSy) chemistry climate model with T42 horizontal truncation. It has 74 levels in the vertical direction and covers an altitude up to 220 km. The neutral chemistry and the ion-chemistry model are calculated iteratively as follows:

1. The neutral model is time dependent and calculates the volume mixing ratios of the neutral species with a variable time step and feeds them to the ion-chemistry model.

2. The ion-chemistry in the equilibrium state is calculated, calling it hourly from the neutral model. The highest level for which the ion-chemistry is calculated is 1 (207.4 km) and the lowest level is 53 (25.4 km), which depends on the initialisation.

3. The net effective production or loss rates of neutral species due to primary ionization, positive and negative ion-chemistry which can also be used as a parameterisation for global chemistry-climate models(Nieder et al., 2014), are computed using an iterative chemical equilibrium approach.

https://doi.org/10.5194/egusphere-2023-427
Preprint. Discussion started: 13 March 2023

4. The production rates resulting from the ion-chemistry computation are then fed back to the 1-D neutral chemistry model, which solves for the neutral atmospheric state transiently using the net effective production/loss reactions as well as neutral photo-chemistry reactions.

5. Lastly, this state is again returned to the ion-chemistry model for the following computation.

The model settings used for the sensitivity studies were mainly variations of full ion-chemistry containing both positive and negative ions from the D-region: setting reactive $O(^1D)$ in photo-chemical equilibrium and switching off the chlorine ion-chemistry. Parameterised NO_x and HO_x model simulations based on Porter et al. (1976) and Solomon et al. (1981) were also carried out to assess the performance of the full ion-chemistry model.

2.2.1 Full-ion chemistry

The ionisation in this case is driven by prescribed ionisation rates and by photo-ionisation of NO, with the primary positive charges being distributed onto N_2, N, O_2 and O and balanced with electrons (Sinnhuber et al., 2012). The ionisation of CO_2 was recently included. These rates of the primary ions are calculated by ionisation cross-sections based on Rusch et al. (1981) and Jones and Rees (1973). All of the processes like dissociation and dissociative ionisation of O_2 and N_2 as well as ionisation of O_2, N_2 and O can form the excited states of N, O, N_2^+, N^+, NO^+ which are also included in the model. More details with a full list of the reactions, reactions rates and references for the reactions rates used for the positive ion-chemistry can be found in Sinnhuber et al. (2012) and the newer versions in Herbst et al. (2022).

2.2.2 Full-ion chemistry with $O(^1D)$ in photo-chemical equilibrium

$O(^1D)$ is a reactive species which is formed from the dissociation of O_2 and CO_2 by particle impact ionisation but also in the ion-chemistry reactions itself. It generally goes into photo-chemical equilibrium but that is not considered in the ion-chemistry part of the model, so the rate of $O(^1D)$ formation passed to the neutral chemistry is too large. There are a few other short lived neutral species in the ion-chemistry model, like the excited states of N that are also treated like ions. Since $O(^1D)$ is short lived mostly but not considered to go into equilibrium in the ion-chemistry stage, a large rate of formation of $O(^1D)$ is produced and added to the neutral chemistry. $O(^1D)$ can react with species like H_2O, H_2 and CH_4 in the lower stratosphere and also with HCl in the stratosphere to produce OH. Therefore, setting either the formation rates of $O(^1D)$ to zero or calculating it in photo-chemical equilibrium significantly makes a difference to the full ion-chemistry through reactions R40, R41, R42 and R43.

$$O(^1D) + H_2O \longrightarrow 2OH \quad \text{(R40)}$$

$$O(^1D) + H_2 \longrightarrow OH + H \quad \text{(R41)}$$

$$O(^1D) + CH_4 \longrightarrow CH_3 + OH \quad \text{(R42)}$$

$$O(^1D) + HCl \longrightarrow OH + Cl \quad \text{(R43)}$$

https://doi.org/10.5194/egusphere-2023-427
Preprint. Discussion started: 13 March 2023

2.2.3 Sensitivity tests switching off the chlorine ion-chemistry

The purpose of this sensitivity test is to study the impact of the chlorine ion, an important negative ion in the lower D region. We also wanted to study what difference it makes to the full ion-chemistry with a focus on the ozone loss. This is done by switching off the reactions of negative chlorine ions with neutrals or the recombination reactions with H^+ in ExoTIC. The relevant reactions are given in Table A1.

2.2.4 Parameterised NO_x and HO_x

The assumption in case of parameterised NO_x is that 1.25 N atoms are produced per ion pair when electrically charged particles collide and dissociate N_2. This process produces N_2^+ and NO^+ ions and, finally, atomic nitrogen. The latter is produced in its ground state N(^{4}S) (45 % or 0.55 per ion pair) and the excited state N(^{2}D) (55 % or 0.7 per ion pair). These values are mostly used in stratospheric and mesospheric models. In case of HO_x, each ion pair typically results in the production of around two HO_x constituents, i.e. a pair of H and OH per ion pair during recombination of the protonised water cluster ions in the upper stratosphere and lower mesosphere (Reaction R5) which was first estimated by Swider and Keneshea (1973).

2.3 MIPAS on ENVISAT

The Michelson Interferometer for Passive Atmospheric Sounding (MIPAS) was a Fourier transform spectrometer for the detection of mid-infrared limb emission spectra in the middle and upper atmosphere on the Envisat (Environmental Satellite, 2000) mission (Fischer et al., 2008). ENVISAT was launched in 2002 into a sun-synchronous polar orbit (800 km) and stopped operation in April 2012. The atmospheric spectra were inverted into vertical profiles of atmospheric pressure, temperature and volume mixing ratios (vmrs) of more than 30 trace constituents. MIPAS observed a spectral range of 4.15 μm to 14.6 μm with a high spectral resolution, where a wide variety of trace gases have absorption lines and signals that are generally higher than in other parts of the spectrum. This is because the Planck function maximises at about 10 μm for atmospheric temperatures. The measurement strategy of the MIPAS instrument was based on trace gases having characteristic emission and absorption lines, represented by their absorption coefficients, which are unambiguous "fingerprints" of the particular trace gases. The MIPAS mission is separated into two phases, caused by a malfunction of the instrument around March 2004. The first phase of the mission (2002–2004) is usually referred to as the MIPAS full-resolution (FR) period. After the malfunction, operation was resumed with a reduced optical path difference, resulting in deteriorated spectral resolution. The second phase starting in January 2005 is called the reduced-resolution (RR) period. Because of the long optical path through the atmospheric layers, MIPAS could also detect trace gases with very low mixing ratios. Vertical information was gained by scanning the atmosphere at different elevation angles with different tangent altitudes. MIPAS could observe atmospheric parameters in the altitude range from 5 to 68 km nominally with minimum and maximum vertical steps of 1 and 8 km respectively. The MIPAS data are used here for evaluation of the model results with different parameterisations. Data presented here are IMK version V5 data for HOCl, ozone, $ClONO_2$ and NO_y species (NO, NO_2, HNO_3, N_2O_5), which are updates of those published by von Clarmann et al. (2006), von Clarmann et al. (2012), Glatthor et al. (2006), Höpfner et al. (2007) and Funke et al. (2005b).

https://doi.org/10.5194/egusphere-2023-427
Preprint. Discussion started: 13 March 2023

2.3.1 Averaging Kernels

Different vertical resolutions of the MIPAS observations and the model need to be accounted for a meaningful comparison. The ExoTIC model has a vertical resolution of 2.7 km whereas MIPAS has different vertical resolutions for different species. For example, in case of HOCl, the maximum vertical resolution can be 17 km and for $ClONO_2$, it can be 13 km at an altitude of 40 km and above as seen from an example Figure 2 for a specific time point.

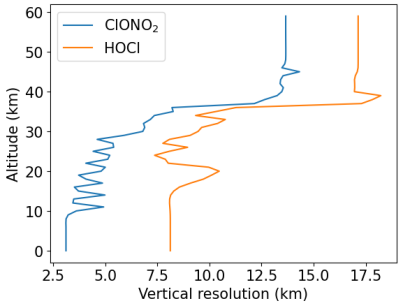

Figure 2. Example of typical profiles for the vertical resolution of HOCl and $ClONO_2$

To remove the discrepancy of different vertical resolutions between the model and MIPAS observations, the original model profiles have to be convolved and adjusted to the MIPAS altitude resolution. This adjustment procedure yields new species profiles that MIPAS would see if it were to sound the model atmosphere. For this purpose, we make use of the averaging kernels (Rodgers, 2000) and use a scheme suggested by Connor et al. (1994) to adjust the better resolved model profiles to those of MIPAS and the new adjusted model profiles x_{new} are calculated as:

$$x_{\mathrm{new}} = \mathbf{A}x_{\mathrm{orig}} + (\mathbf{I} - \mathbf{A})x_{\mathrm{a}} \tag{1}$$

where $\mathbf{A}$ is the MIPAS averaging kernel matrix, x_{orig} is the original model profile, $\mathbf{I}$ is a unity matrix and x_{a} is the a priori information used in the MIPAS retrievels. The rows of the AK matrix give the contribution of the true values to the retrieved values and the columns give the response of the delta peak like perturbations at each altitude. Figure 3 shows an example of averaging kernels for the different species and for a profile retrieved from spectra measured at latitude of 67.5°N on 27 October 2003 at 00:00 UT. From the figure, it is seen that the trace gas retrievals result in different sensitivities at different altitudes. For example, the maximum sensitivity is seen at 20 km for HOCl in this specific case, whereas for $ClONO_2$, it is around 15 km. To characterize the vertical resolution, the typical measures are either the full width at half maximum of the rows of the $\mathbf{A}$ or the gridwidth divided by the respective diagonal of $\mathbf{A}$ (Rodgers, 2000).

https://doi.org/10.5194/egusphere-2023-427
Preprint. Discussion started: 13 March 2023

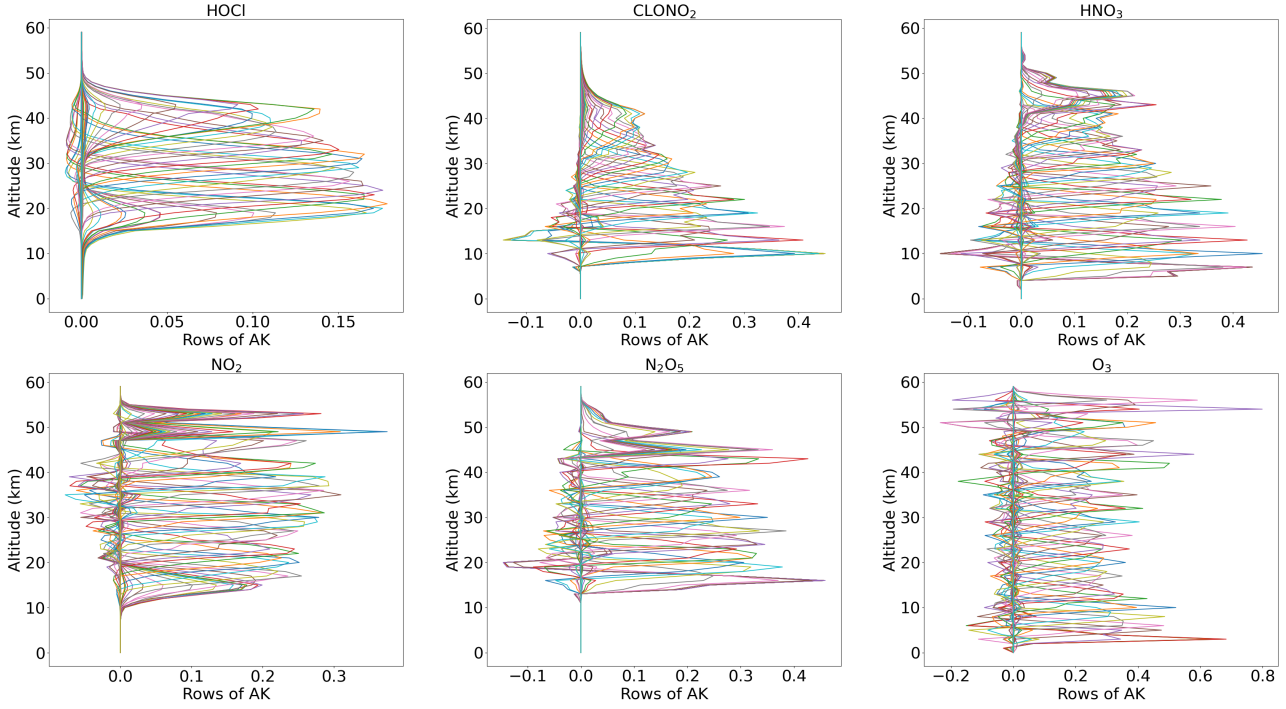

Figure 3. Example of rows of averaging Kernels for typical MIPAS HOCl, $ClONO_2$, HNO_3, NO_2, N_2O_5 and O_3 at a latitude of 67.5°N on 27 October 2003 at 00:00 UT.

3 Comparison of ExoTIC simulations to MIPAS observations for the Halloween SPE 2003

In this section, a comparison study between the ExoTIC model results and MIPAS observations has been carried out for the chlorine species of HOCl, $ClONO_2$, ozone and odd oxides of nitrogen (NO_y) for the Halloween SPE 2003. The comparison is done for the model simulations with different settings of ion-chemistry, i.e. calculating the photo-chemical equilibrium of $O(^1D)$ and switching off the uptake of chlorine ions, and parameterised NO_x and HO_x. The model simulations are performed for a high latitude of 67.5° N and the MIPAS data were taken for the polar cap region, averaged over geographic latitudes such that it's inside the vortex, either vortex core or vortex edge depending on the tracer properties. The model data is sampled in the MIPAS altitude grid as well. The day and night for the MIPAS data are sorted according to the solar zenith angle (day $\leq$ 90°; night $>$ 98°). The solar zenith angles for the 1D model were chosen such that, for each day, it is the mean solar zenith angle for the MIPAS data plus/minus the standard error of mean (SEM) with N being the number of data points for each day.

$$\text{SEM} = \frac{\text{Standard Deviation}}{\sqrt{\text{N}}} \tag{2}$$

Since ExoTIC doesn't have diffusion or horizontal and vertical transport, the comparison can only be done for a short period of time. The model results are compared with the MIPAS observations for a total of 9 days from 26$^{\text{th}}$ October to 3$^{\text{rd}}$ November 2003. Due to different vertical resolutions between the model and MIPAS observations, averaging kernels were applied. Now,

https://doi.org/10.5194/egusphere-2023-427
Preprint. Discussion started: 13 March 2023

ExoTIC being a 1D column model doesn't produce the output at the same geolocations as MIPAS hence the application of the MIPAS averaging kernels was based on the temperature criteria. The following procedure was applied for the convolution:

1. The model profile from the time series was fixed first.
2. All the profiles from MIPAS within 57.5 and 77.5 degrees latitude and +/- 6 hours of the model profile's time were selected.
3. For this obtained MIPAS sample of temperature profiles, the root mean square value was calculated with the model's temperature profile which is fixed for the entire time series.
4. The geolocation for which the root mean square value of the temperature difference profile was minimal was selected, and averaging kernels for this geolocation were applied to the trace gas profiles from the model.

Using this procedure, we have obtained model profiles that were adjusted to the vertical resolution of MIPAS. The data was then averaged daily and the absolute or relative differences w.r.t a day before the event, i.e. 26^{th} October 2003 (day 299), was calculated.

3.1 Estimation of the polar vortex edge

There are different methods of estimating the vortex edge and one of the methods widely used is using CO as a tracer of vortex air. Due to its strong vertical gradient and longevity in the polar winter vortex, carbon monoxide is commonly used as a tracer of vortex air originating from the upper mesosphere and lower thermosphere, which is transported down into the lower mesosphere and stratosphere in the polar vortex. Hence it can be used to estimate the vortex edge. Funke et al. (2005a) also used the CO gradient for the vortex boundary definition, which is less dependent on the actual conditions, and also in their case the maximum derivative was around 0.5 ppmv. Figure 4 shows volume mixing ratios of CO versus latitude in the Northern Hemisphere for different longitude bins of size 20 (shown by different colours) and averaged over latitude bins of size 5 from 27^{th} October (day 300) to 3^{rd} (day 307) November 2003 separated by day-time and night-time. Choosing a threshold of 0.5 ppm of CO, the edge of the polar vortex can be determined from the corresponding x-axis where an increase of the volume mixing ratios start to occur. An increase is observed starting at a latitude of approximately around 55° N for the different days. The estimation of the polar vortex edge helps to choose the MIPAS sampling of the zonal averages for a better inter-comparison.

https://doi.org/10.5194/egusphere-2023-427
Preprint. Discussion started: 13 March 2023

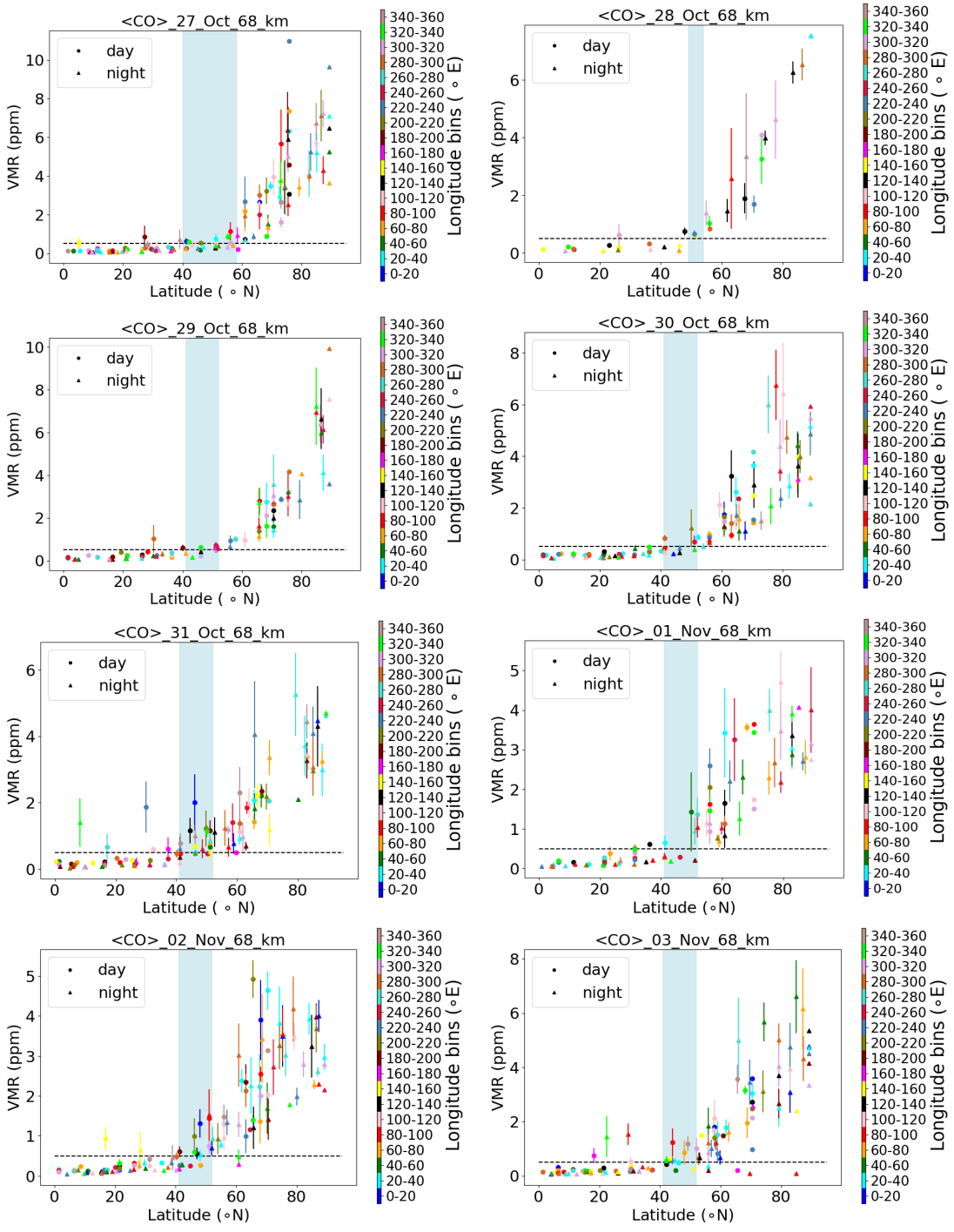

Figure 4. MIPAS CO (ppm) as a function of latitude (° N) for longitude bins of size 20 and averaged over latitude bins of size 5 for 27th October- 3rd November 2003 (day and night) at 68 km altitude. Colors mark the longitude bins from 0-20 °E to 340-360 °E running from blue to rosybrown. The error bars mark the standard error of mean. The light-blue shaded region marks the latitude range of the vortex edge and the dashed horizontal line is the CO threshold of 0.5 ppm.

https://doi.org/10.5194/egusphere-2023-427
Preprint. Discussion started: 13 March 2023

3.2 HOCl change

A comparison of Envisat MIPAS V5_HOCl measurements for the polar Northern Hemisphere (57-77° N) and ExoTIC computations with different settings of HOCl simulation is presented in Figure 5 for daytime and night-time. The model and the MIPAS data are sampled on the MIPAS altitude grid and the model is read out in the solar zenith angle range of MIPAS daytime and night-time observations. The values in Figure 5 start on the 26th October 2003 (day 299). MIPAS observations for HOCl showed significant enhancements with peak values of 0.2 ppb for daytime and 0.24 ppb for night-time on the 29th of October. The model results with full-ion chemistry significantly overestimated the observed enhancements for night-time by a factor of 4 (around 1.25 ppb), and for day-time by a factor of 3 (around 0.65 ppb) produced at an altitude of 35-40 km. HOCl enhancements below 30 km was also observed for both daytime and night-time with full ion-chemistry and a peak producing 0.12 ppb was observed in the mesosphere during night-time. Sensitivity studies were performed setting O(^{1}D) to photo-chemical equilibrium that showed a decrease in the enhancements from 1.25 ppb to 0.55 ppb during night-time and 0.65 ppb to 0.08 ppb during daytime produced by the model also at 35-40 km during the event. The higher mixing ratios of HOCl below 30 km for both daytime and night-time also disappeared with this setting. Switching off the chlorine ion-chemistry led to the removal of the peak of 0.2 ppb observed in the mesosphere during night-time. And similar behaviour was also observed for the parameterised NO_x and HO_x model. However, significantly low values were observed during daytime for the model, setting O(^{1}D) to photo-chemical equilibrium, without chlorine ion-chemistry and parameterised NO_x and HO_x. Reaction rate constants and photo-chemical data follow in general the JPL-2006 recommendations from Sander et al. (2006).

After the application of averaging kernels the higher mixing ratios produced by the model were significantly smeared out over altitudes and reduced in their peak value. For daytime, the peak value of the full ion-chemistry model decreased from 0.65 ppb to 0.4 ppb. And for the sensitivity studies with O(^{1}D) in photo-chemical equilibrium, without chlorine ion-chemistry and parameterised NO_x and HO_x, the peak value of 0.08 ppb decreased to 0.03 ppb. For night-time, full ion-chemistry peak value of 1.25 ppb went down to 0.84 ppb after applying the MIPAS averaging kernels. Setting O(^{1}D) to photo-chemical equilibrium decreased the peak value from 0.55 ppb to 0.36 ppb which is in better agreement with the MIPAS observations. For the model without chlorine ion-chemistry and parameterised NO_x and HO_x, the enhancements of 0.58 ppb went down to 0.33 ppb which also agrees quite well. Jackman et al. (2008) also compared results from the Whole Atmosphere Community Climate Model (WACCM3) with MIPAS observations and applied MIPAS averaging kernels for the Halloween SPE 2003. They found the HOCl peak at an altitude of 48 km on the 29th of October and the MIPAS averaging kernels moved it down to 40 km. ExoTIC however produced the peak around 35-40 km itself for both daytime and night-time for all the test cases. This is actually quite in agreement with the MIPAS observations and the application of the averaging kernels also didn't shift the peak in terms of altitude. This difference in the peak altitude between the results from Jackman et al. (2008) and ExoTIC might be due to the fact that WACCM3 has fully interactive dynamics, radiation, chemistry and other parameterizations whereas ExoTIC includes only the chemistry. Damiani et al. (2012) considered the SPE of January 2005 where they observed 0.2 ppb increase of HOCl during the event in the polar cap region also using the WACCM model that agreed quite well with Microwave Limb Sounder (MLS) observations. Enhancements of HOCl results from enhanced HO_x constituents. In the middle stratosphere, it is mainly

https://doi.org/10.5194/egusphere-2023-427
Preprint. Discussion started: 13 March 2023

accelerated by odd hydrogen chemistry (via Reaction R8). The morphology of the HOCl distribution and it's temporal variation is a combined effect of photolysis, temperature and availability of ClO, HO_2 and OH, which in themselves show pronounced diurnal variation.

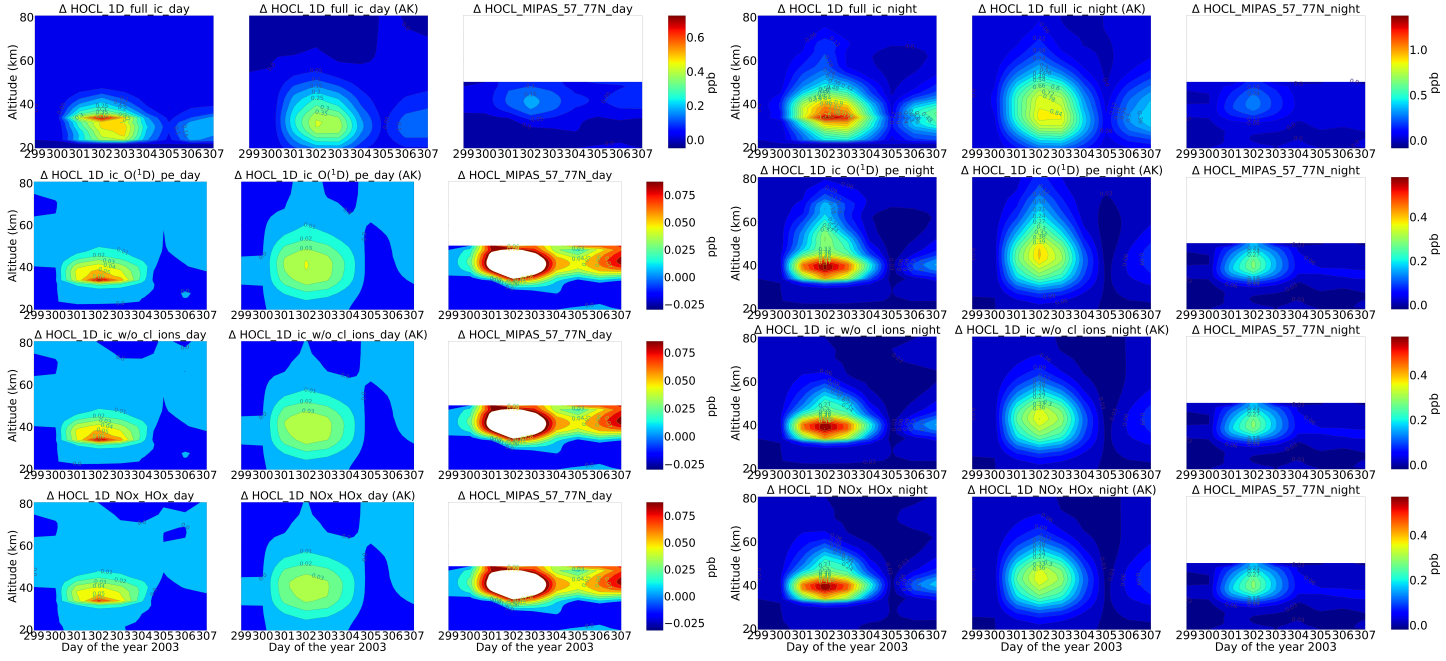

Figure 5. Absolute differences of daily averaged data for HOCl w.r.t. a day before the event, i.e. 26th October 2003. Starting point is 26th October 2003 and for the four different model settings (row-wise: full ion-chemistry, full ion-chemistry with O(^{1}D) in photochemical equilibrium, without chlorine ion-chemistry and parameterised NO_x and HO_x); column-wise: without AK, with AK applied and MIPAS observations averaged over 57-77° N for day-time (sza <= 90°) (left) and night-time (sza > 98°) (right). Colorbar is adjusted to the first plot in all the rows for both daytime and night-time. For daytime, the white region in the MIPAS peak (0.2 ppb) is because the colorbar for the second, third and fourth rows are adjusted to the lower mixing ratios predicted by the model (first plot). The white region above 50 km for the MIPAS observations represent meaningless data, where the values of AK diagonal elements are close to zero (< 0.03) that indicate no significant sensitivity to the retrieved parameter at the corresponding altitude.

3.3 $ClONO_2$ change

Figure 6 shows the daily averaged absolute differences for chlorine nitrate w.r.t. 26th October 2003 for day-time and night-time. The zonal average for $ClONO_2$ observations was also taken over a latitude range of 57-77° N, which is at the edge of the polar vortex. Continuous enhancements of $ClONO_2$ is observed for the full ion-chemistry model with peak values of 0.96 ppb and 1.15 ppb also approximately two days after the event for daytime and night-time respectively starting from the onset of the event on 28th of October. The peak was observed around 25 km. In case of the model with full ion-chemistry but O(^{1}D) in photo-chemical equilibrium, a peak value of around 0.18 ppb was observed for both day-time and night-time which compared much better with the MIPAS observations. Similar results were also observed for the sensitivity study without

https://doi.org/10.5194/egusphere-2023-427
Preprint. Discussion started: 13 March 2023

chlorine ion-chemistry and parameterised NO_x and HO_x model. The increase was seen also approximately two days after the event in the altitude range of 35-40 km. After the application of averaging kernels the peak value for the full ion-chemistry daytime and night-time decreased down to 0.66 ppb and 0.78 ppb respectively. For the rest, the peak value decreased from 0.12 ppb to 0.09 ppb for daytime and from 0.18 ppb to 0.12 ppb for night-time. Jackman et al. (2008) observed $ClONO_2$ maximum enhancements of 0.3-0.4 ppb with the peak production at a higher altitude of 40-45 km with WACCM3. The peak however was produced several days later than MIPAS. The application of MIPAS averaging kernels moved the peak down to 40 km and the predicted peak increases are reduced substantially to about 0.2 ppbv, about a factor of 2 less than MIPAS observations.

The enhanced $ClONO_2$ production happens due to SPE produced NO_x via reaction R13. $ClONO_2$ is removed mainly by photolysis in the sunlit atmosphere and, to a lesser extent, by reaction with atomic oxygen. And due to it's pressure dependence, $ClONO_2$ formation by Reaction R13 is more effective at lower altitudes (Funke et al., 2011). The zonal average of MIPAS observations were tested for latitude bands 57-77° N, i.e., at the edge of the polar vortex and 70-90° N, deep in the polar vortex. The sample of 57-77° N works better for the inter-comparison of $ClONO_2$ compared to 70-90° N. In case the sample is taken deep in the vortex, the model seemed to fairly underestimate the peak values. This can be explained by the reaction R13, where formation of ClO needs sunlight, which is available more at the edge of the polar vortex. But $ClONO_2$ can also photolyse in the presence of sunlight. Due to this, there is a balance between the two processes and $ClONO_2$ can form at the edge of the polar vortex which can be transported deep into the vortex and conserved there at high latitudes. This however cannot be reproduced by the 1D model because it is fixed at a certain location and has no transport.

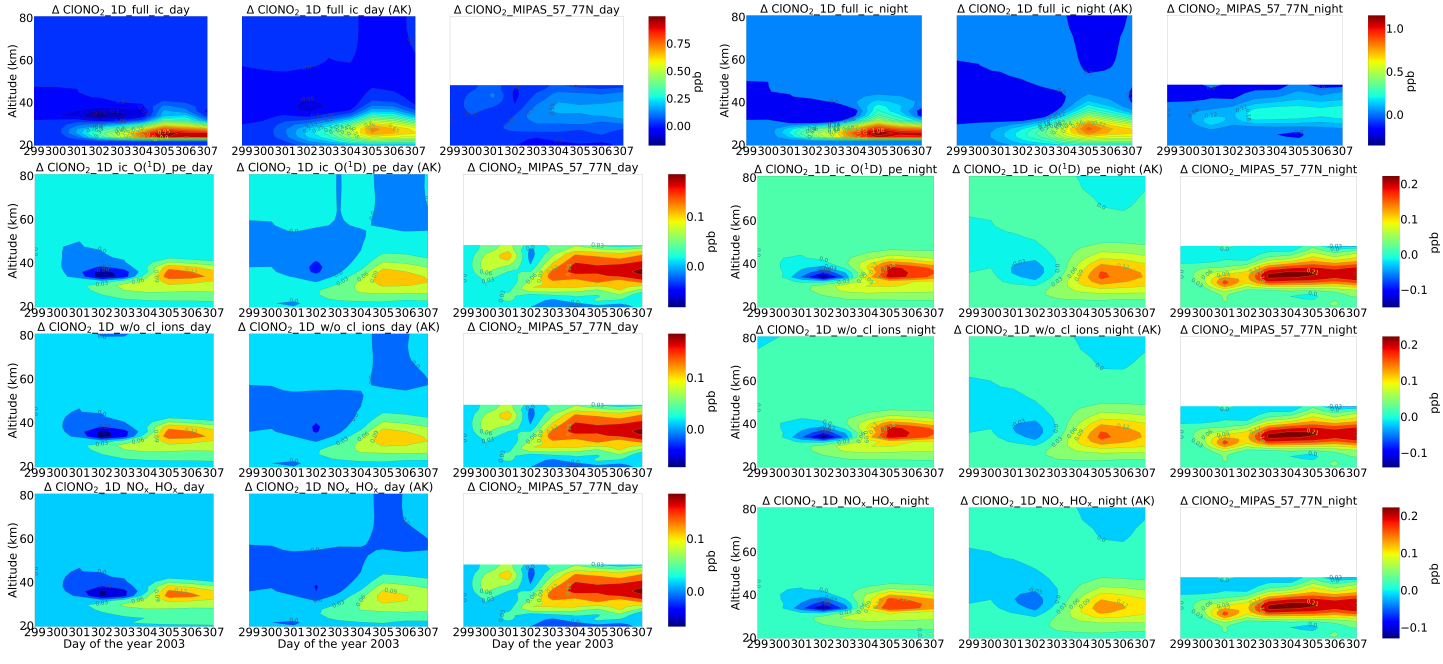

Figure 6. Same as Figure 5 but for $ClONO_2$. The colorbars for the first row are adjusted to the first plot. For the second, third and fourth rows, the colorbar is adjusted to the third plot for both day-time (left) and night-time (right).

https://doi.org/10.5194/egusphere-2023-427
Preprint. Discussion started: 13 March 2023

3.4 Odd oxides of nitrogen (NO_y)

An important impact of proton precipitation in the middle atmosphere is the formation of NO_x which happens by the dissociation of molecular nitrogen by ionisation and subsequent recombination with oxygen. In order to assess the agreement of the observed and modelled SPE related odd nitrogen enhancements, total NO_y (=NO + NO_2 + HNO_3 + $2N_2O_5$ + $ClONO_2$) is compared. The observed and modelled NO_y enhancements w.r.t. 26^{th} October is shown in figure 7 for daytime (left) and night-time (right) conditions respectively. Averaging kernels are also applied to the model profiles for the different NO_y species for the different model settings and then added, except for NO. In case of MIPAS NO and NO_2 data, there is a complication which is, that instead of mixing ratios the logarithms of the mixing ratios are retrieved; also the averaging kernels refer to the logarithms of the mixing ratios. The application of MIPAS averaging kernels to a better resolved profile on the basis of the coarse-grid averaging kernel **A** of the logarithm of the mixing ratio then is (Stiller et al., 2012):

$$x_{\mathrm{new}} = \exp(\mathbf{A}\log(x_{\mathrm{orig}}) + (\mathbf{I} - \mathbf{A})\log(x_{\mathrm{a}})) \quad (3)$$

There is a general issue with logarithmic retrievals, because regularization is self-adaptive and depends on the actual state of the atmosphere. For an SPE response, if the NO peaks around 50-60 km and if there is a better sensitivity at this altitude the Jacobian and the averaging kernels scale with the volume mixing ratio. For NO_2 however, the logarithmic averaging kernels behave well and are not dependent on the actual conditions (for a deeper discussion of the problem of time and state dependent averaging kernels, see von Clarmann et al. (2020)). Due to this complication, for the total NO_y in the second column of figure 7 for both daytime and night-time, NO is added without the application of the averaging kernels as compared to the rest of the species.

The magnitude of NO_y enhancements is found to be larger for the ExoTIC model with ion-chemistry settings compared to the MIPAS observations for both daytime and night-time. However the SPE induced NO_y layer is reproduced well in terms of vertical distribution. The MIPAS observations showed a production of 30-40 ppb in the upper stratosphere during night-time and 20-30 ppb during day-time. The results are shown upto 50 km since above 50 km NO is the largest contributor and averaging kernels are not applied to NO. Another reason is that large uncertainties of small vmr values of $ClONO_2$ will spoil the NO_y sum and it's uncertainty. The night-time results compare better with the observations, specially for the parameterised NO_x and HO_x model. For day-time, the model with and without AK didn't make too much of a difference because NO was added without AK and was abundant during daytime.

https://doi.org/10.5194/egusphere-2023-427
Preprint. Discussion started: 13 March 2023

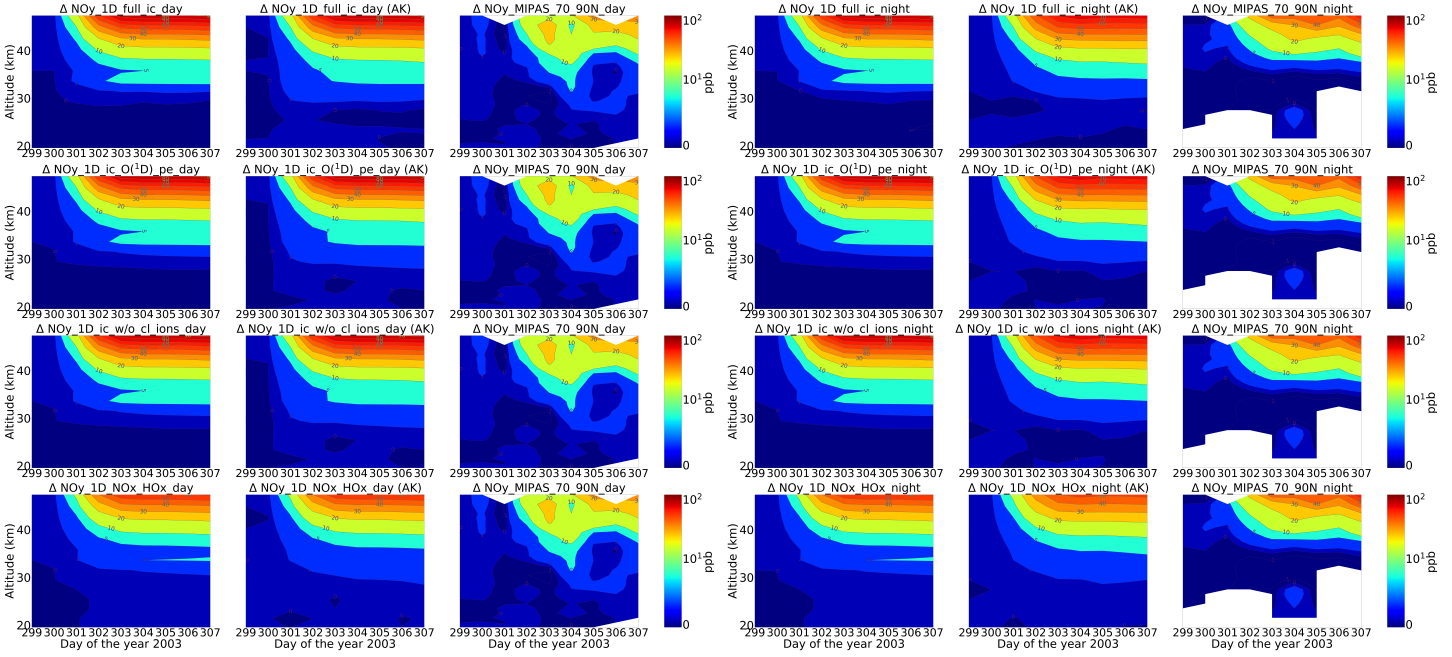

Figure 7. Same as figure 6 but for NO_y species.

3.5 Ozone

Energetic particles in the polar atmosphere enhances the production of NO_x and HO_x in the winter stratosphere and mesosphere. Both NO_x and HO_x are powerful ozone destroyers. An important aspect in the evaluation of the ability of models is the reproduction of the observed ozone destruction caused by the catalytic cycles of NO_x and HO_x during SPE induced chemical composition changes. As inferred from observations, stratospheric ozone decreases due to the indirect effect of EPP by about 10–15 % as observed by satellite instruments. López-Puertas et al. (2005) found HO_x related mesospheric ozone losses upto 70 % and NO_x related stratospheric loss of around 30 % during the Halloween SPE.

Figure 8 shows observed and modelled temporal evolution of the relative ozone changes w.r.t. 26th October, averaged over 70-90°N for daytime (left) and night-time (right). For ozone, the long term history of air parcels is more important as air parcels that are ozone depleted gets dispersed into the mid-latitudes if they are at the edge of the vortex. So a sample deeper in the vortex for ozone is better, the reason we chose 70-90°N here. A loss of 60-75 % is observed during the event itself in the mesosphere that is short lived and is related to the HO_x catalytic cycle (Reactions R14, R15, R17 and R18). The ozone recovers after the event, since HO_x is short-lived. A second peak is observed on the 3rd of November which is related to a weaker coronal mass ejection event. NO_x related loss of 15 % is observed in the stratosphere that lasts longer and is also related to the polar winter atmosphere (Reactions R20 and R21). The full ion-chemistry shows an ongoing loss of 45 % starting from the event day and the sensitivity study with O(^{1}D) in photo-chemical equilibrium confirmed that this loss is due to reactions like R43 and R40, which produces OH and Cl contributing further to ozone loss. The agreement between the observations and

https://doi.org/10.5194/egusphere-2023-427
Preprint. Discussion started: 13 March 2023

the model results, for night-time, for the three model results except for the full ion-chemistry is excellent in the mesosphere indicating a good ability of the model to reproduce HO_x related ozone loss for SPEs. However, the ozone loss shifted to lower altitudes for both daytime and night-time in all the model settings as compared to MIPAS observations. This could be explained as a result of the AISstorm ionisation rates that was used in the model which could be different to what MIPAS might have experienced during the SPE.

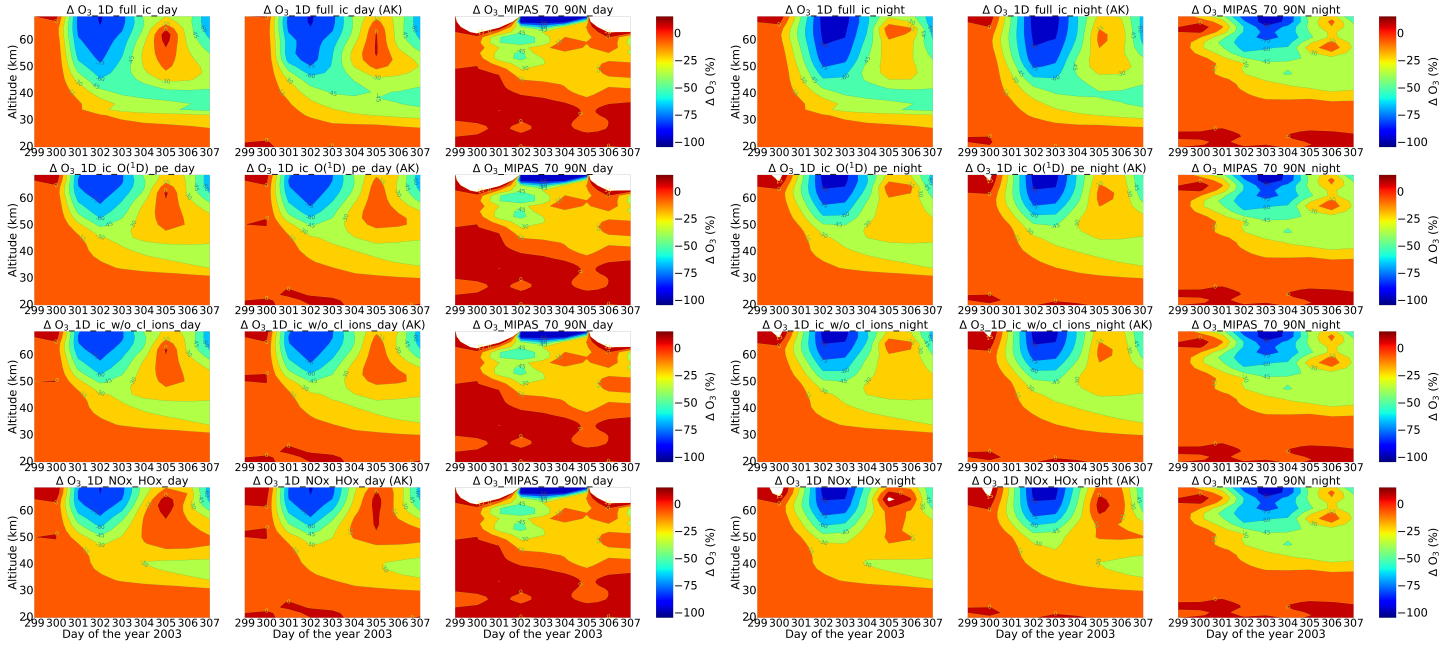

Figure 8. Relative difference of ozone w.r.t. 26$^{\text{th}}$ October. Rest is same as Figure 6.

4 Comparison of the Halloween storm and the extreme solar event of 775 A.D.

In this section, a comparison study between the Halloween storm of 2003 and an extreme event of 775 A.D. is presented. The model simulations begin at the noon of 27$^{\text{th}}$ October (day 300) and the ionisation rate profiles obtained from AISstorm for both the events are input from the noon of October 28 to noon of October 29. Since the studies were performed without horizontal and vertical transport, the results shown here are restricted to a short time period. The results are shown for the model simulations for the settings that compared well with MIPAS observations.

4.1 $N\tilde{O}_y$ and HO_x:

Figure 9 shows the formation of $N\tilde{O}_y$ during the Halloween SPE and the extreme scenario with different settings of the ion-chemistry. $N\tilde{O}_y$ consists species of odd nitrogen as shown in equation 4:

$$N\tilde{O}_y = NO + NO_2 + N + HNO_3 + 2N_2O_5 + NO_3 + ClONO_2, \quad (4)$$

https://doi.org/10.5194/egusphere-2023-427
Preprint. Discussion started: 13 March 2023

After the onset of the event, $N\tilde{O}_y$ starts accumulating over time in the stratosphere and lower mesosphere. For the extreme scenario, the volume mixing ratio (VMR) of $N\tilde{O}_y$ is about one order of magnitude larger compared to the Halloween SPE in the upper stratosphere and lower mesosphere. For example, the amount of $N\tilde{O}_y$ at 60 km is found to be 50 ppb for the Halloween event compared to 500 ppb for the extreme event. Additionally for the extreme event, $N\tilde{O}_y$ is seen to be formed even in the lower stratosphere (below 30 km). This is because of the high values of ionisation rates that reached further down in altitude in this case. A small difference was observed between the sensitivity study without the chlorine ion-chemistry and the model setting of full ion-chemistry with O(^{1}D) in photo-chemical equilibrium around 75 km. For the parameterised model, $N\tilde{O}_y$ enhancements are observed in the mesosphere and lower thermosphere with higher values seen for the extreme scenario compared to the Halloween event. Since only N, NO and NO_2 are present for the parameterised NO_x, the impact of the scavenging reaction R2 is stronger and the partitioning between N and NO is different compared to the full ion chemistry which also contains other $N\tilde{O}_y$ species like HNO_3 etc. R2 drives the NO_x parameterisation and makes the main difference w.r.t. the ion-chemistry. The HO_x parameterisation doesn't make much of a difference for $N\tilde{O}_y$.

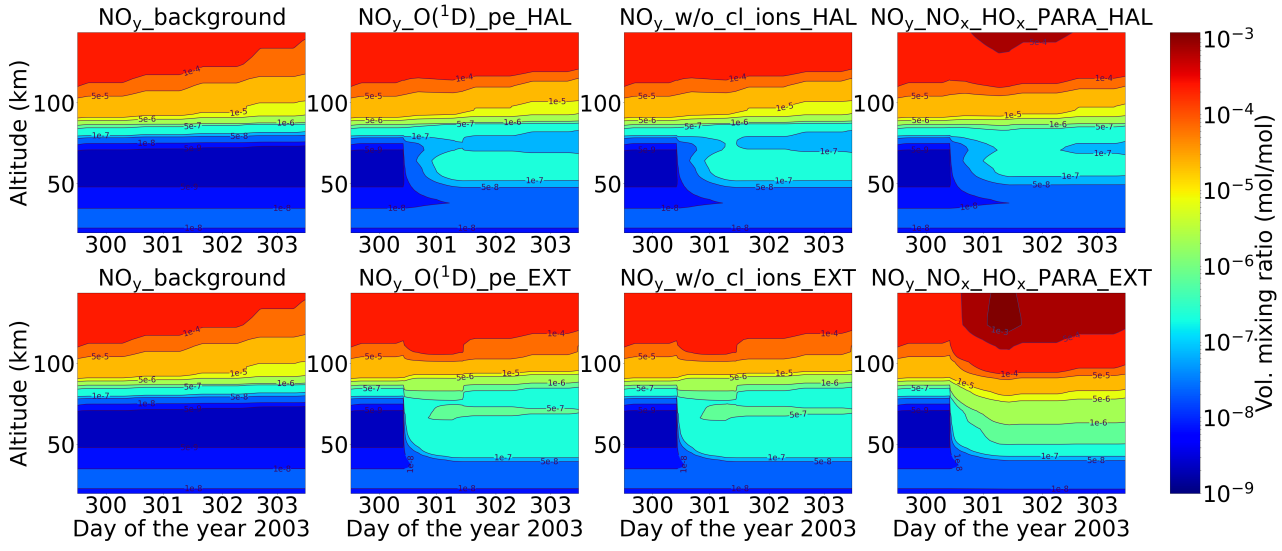

Figure 9. Comparison of the Halloween SPE and the extreme scenario (row-wise) for $N\tilde{O}_y$: reference run (background atmosphere), full ion-chemistry with O(^{1}D) set to photo-chemical equilibrium, without chlorine ions and parameterised NO_x and HO_x model (column-wise) for a high latitude of 67.57° N.

Figure 10 shows the temporal evolution of HO_x for the Halloween SPE and extreme scenario that consists of odd hydrogen species (equation 5);

$$HO_x = H + OH + HO_2 + 2H_2O_2 \tag{5}$$

HO_x enhancements are seen during the event. For the Halloween SPE, significant HO_x enhancements of 0.1 ppm were observed in the mesosphere during the event whereas for the extreme scenario these enhancements were seen to penetrate

https://doi.org/10.5194/egusphere-2023-427
Preprint. Discussion started: 13 March 2023

deep down. However after the event stops, the HO_x disappears at higher altitudes, since it is short-lived up there. But at lower altitudes, around 25-40 km, HO_x enhancements of around 1 ppb was found to be continuous and more persistent, specially for the extreme scenario. The full ion-chemistry shows HO_x enhancements below 30 km which is due to the presence of $O(^1D)$, that can react with water vapour, hydrogen and methane via reactions R40, R41 and R42. However with $O(^1D)$ set to photo-chemical equilibrium, the HO_x enhancements below 30 km disappeared for both the events. The impact of chlorine ion-chemistry is seen to be rather small. For the parameterised model, the recovery of HO_x after the event was found to be slower compared to the ion-chemistry model. The full ion-chemistry with more HO_x can lead to a faster reaction between OH and NO_2 (43), which can produce HNO_3 contributing a difference to the recovery of HO_x.

$$OH + NO_2 \longrightarrow HNO_3 \tag{43}$$

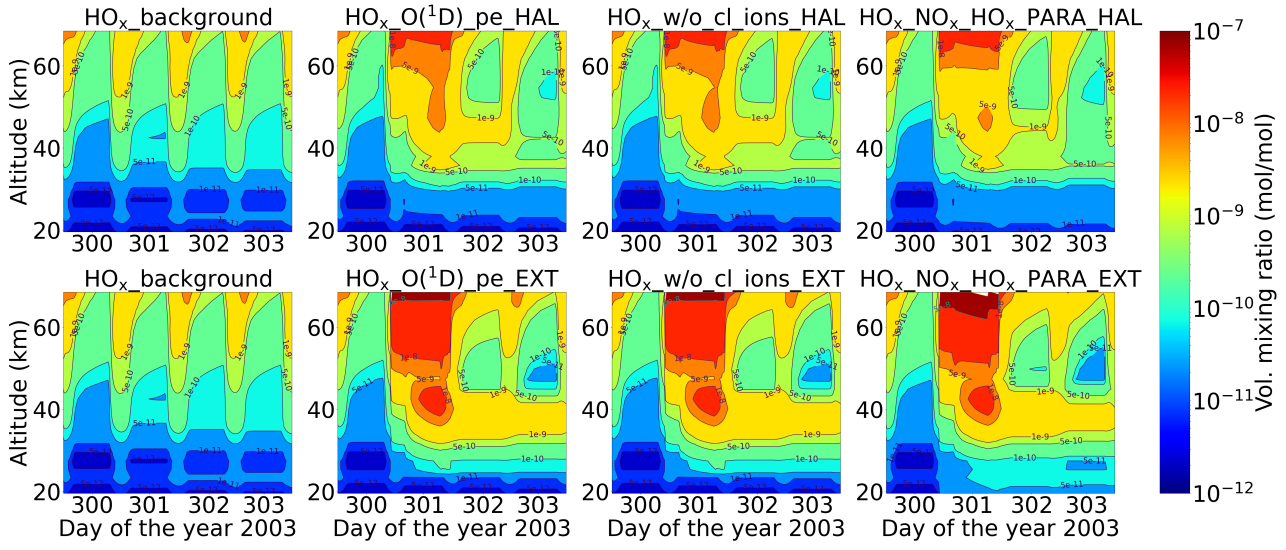

Figure 10. Same as Figure 9 but for odd hydrogen species, HO_x

4.2 Chlorine species:

Figure 11 shows the volume mixing ratios of HCl for the two events. Loss of HCl, which can occur via transformation into reactive chlorine as it is taken up from the gas phase into negative ions, is seen during the event in both cases, pronounced more for the extreme scenario. This occurred both in the stratosphere and the mesosphere for full ion-chemistry. Negative ions upon reaction with HCl can form Cl^- ions, which forms large cluster ions thereby releasing Cl upon recombination (Sinnhuber et al., 2012),

$$HCl + X^- \longrightarrow Cl^- + HX \tag{R44}$$

$$Cl^- + Y \longrightarrow Cl^-Y \tag{R45}$$

$$Cl^-(Y) + Z^+ \longrightarrow Cl + Z + Y \tag{R46}$$

https://doi.org/10.5194/egusphere-2023-427
Preprint. Discussion started: 13 March 2023

where X = O, O_2, CO_3, OH, NO_2, NO_3; Y = HCl, H_2O, CO_2 and Z = positive ions (Kopp and Fritzenwallner, 1997). Cl^- and Cl^- cluster ions like $Cl^-(H_2O)$ can also release HCl via reaction with H (Kopp and Fritzenwallner, 1997). HCl can also react with $O(^1D)$ via reaction R43 resulting in an enhanced loss of HCl below 40 km but that disappears when $O(^1D)$ is set to photo-chemical equilibrium. From the sensitivity study without the chlorine ions, it is evident that the huge loss of HCl observed in the mesosphere is due to the same. The parameterised model underestimates the loss of HCl which was also found in studies by Winkler et al. (2009).

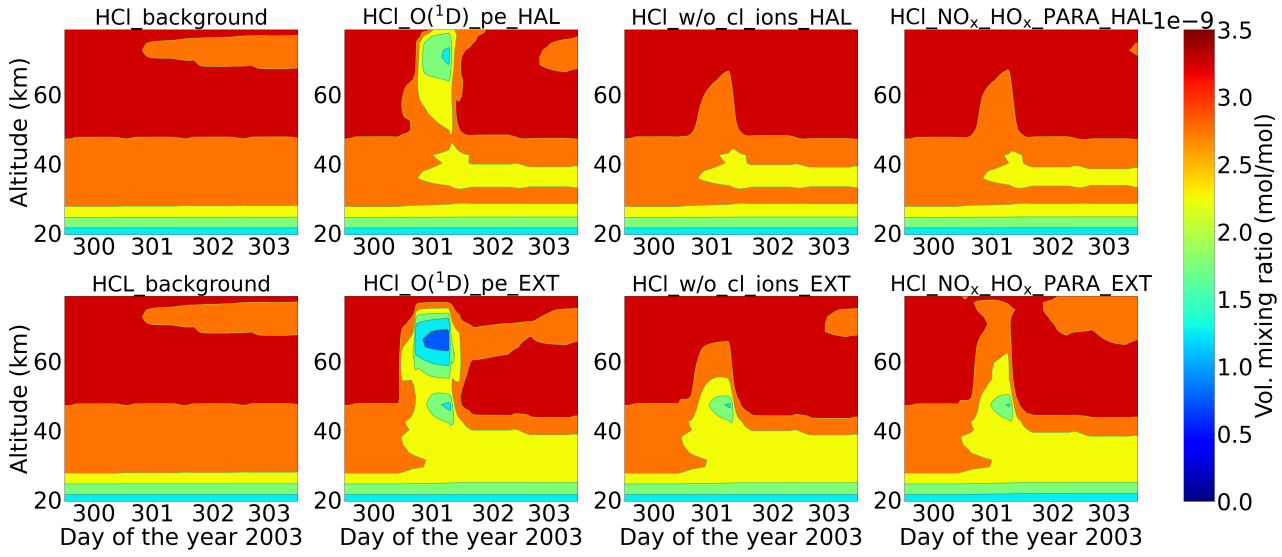

Figure 11. Same as Figure 9 but for HCl

Since $N\tilde{O}_y$ and HO_x production is enhanced during SPEs, which is evident from figures 9 and 10, they can react with reactive chlorine species like ClO. ClO can either react with HO_x producing short term enhancement in HOCl, or with NO_x slowly producing $ClONO_2$. ClO is formed from the reactive Cl via reaction R7 by neutral gas phase reactions of Cl with ozone in the altitude range of 35-40 km. ClO can react with HO_x and NO_x species to form HOCl and $ClONO_2$ (reactions R8 and R13).

From figure 12, it can be seen that ClO decreases during the event for the same altitude range but recovers straight after the event stops. ClO can react with HO_x species during SPEs, particularly HO_2 to produce HOCl (R8), which is also a short-lived species. Therefore, a short term enhancement of HOCl is seen during both the events (Figure 13) which was also observed by von Clarmann et al. (2005) for the Halloween SPE. However for the extreme scenario, loss of ClO continues specially around 30-40 km even after the event stops. This is because of the excess HO_x available for the extreme event, also at the same altitude range, due to which R8 can happen continuously. And loss of HOCl is also seen after the extreme event which is due to excess HO_x as well. HOCl can react with OH to form ClO (R9) and then ClO can react back with HO_2 and this catalytic cycle results in the loss of both species due to excess HO_x.

https://doi.org/10.5194/egusphere-2023-427
Preprint. Discussion started: 13 March 2023

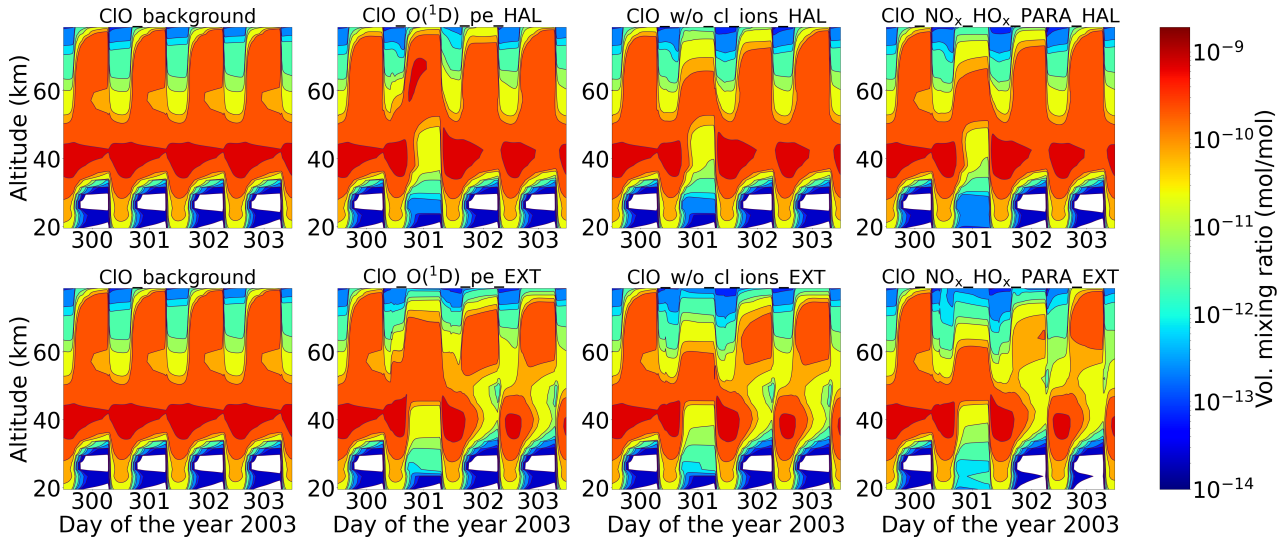

Figure 12. Same as figure 11 but for ClO

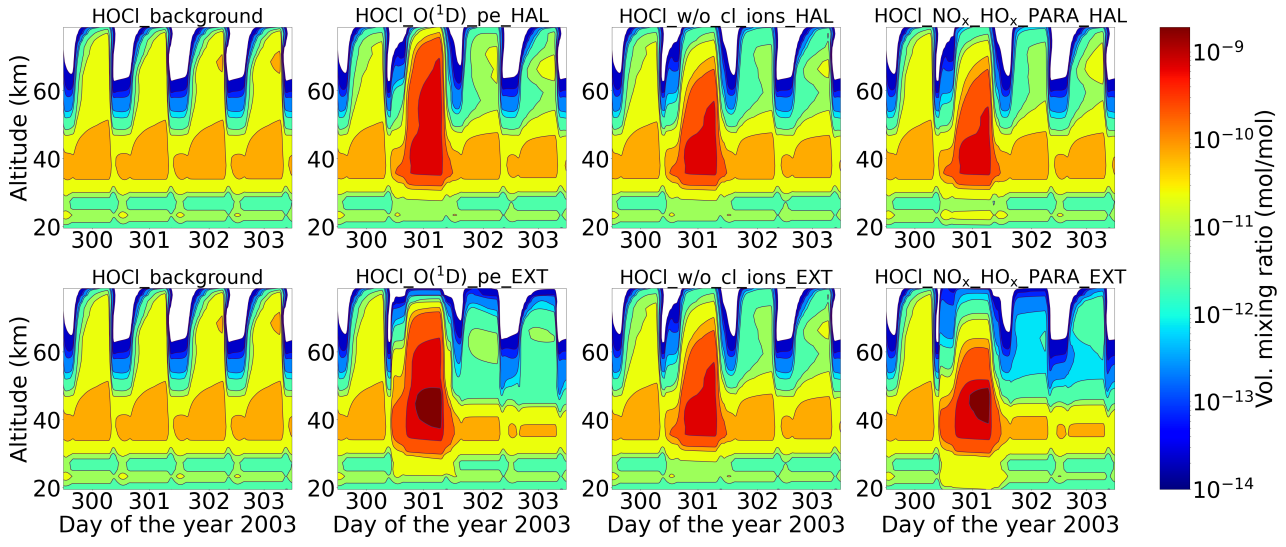

Figure 13. Same as figure 11 but for HOCl

An increase in $ClONO_2$ is also observed during both the events at an altitude of 60 km (Figure 14). Solomon et al. (1981) pointed out that the increasing NO_x concentrations after a SPE interact with chlorine species, forming chlorine nitrate at the expense of reactive radicals. This reaction is of importance in the lower and middle stratosphere around 40 km, (Jackman et al., 2000) but not so important at higher altitudes. It can be seen from Figure 14 that at an altitude of 40 km, $ClONO_2$ increases after the event has stopped. This is because during the event ClO is lost via R8 and NO_x is formed slowly accumulating over

https://doi.org/10.5194/egusphere-2023-427
Preprint. Discussion started: 13 March 2023

time. So the formation of $ClONO_2$ via R13 is slow, hence leading to high production after the event in the lower and middle stratosphere.

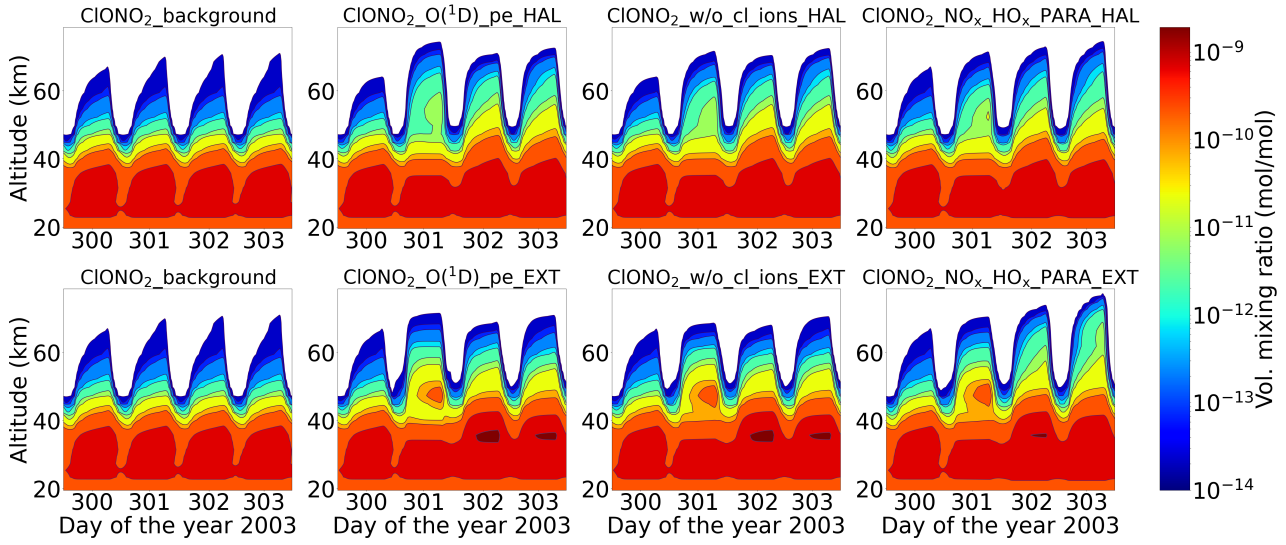

Figure 14. Same as figure 11 but for $ClONO_2$

Figure 15 shows the chlorine species at an altitude of 40 km for the various model set-ups. There is a small impact of chlorine ion-chemistry on the loss of HCl, whereas the parameterised NO_x and HO_x underestimates it. ClO decreases during the event and transfers to HOCl via reaction R8. After the event, it recovers and the HOCl enhancements also decrease. For the extreme event however, ongoing loss of ClO during night-time is observed which is due to the excess HO_x produced during the extreme event. Reformation of HCl after the event is observed that happens via Reactions R11 and R12.

https://doi.org/10.5194/egusphere-2023-427
Preprint. Discussion started: 13 March 2023

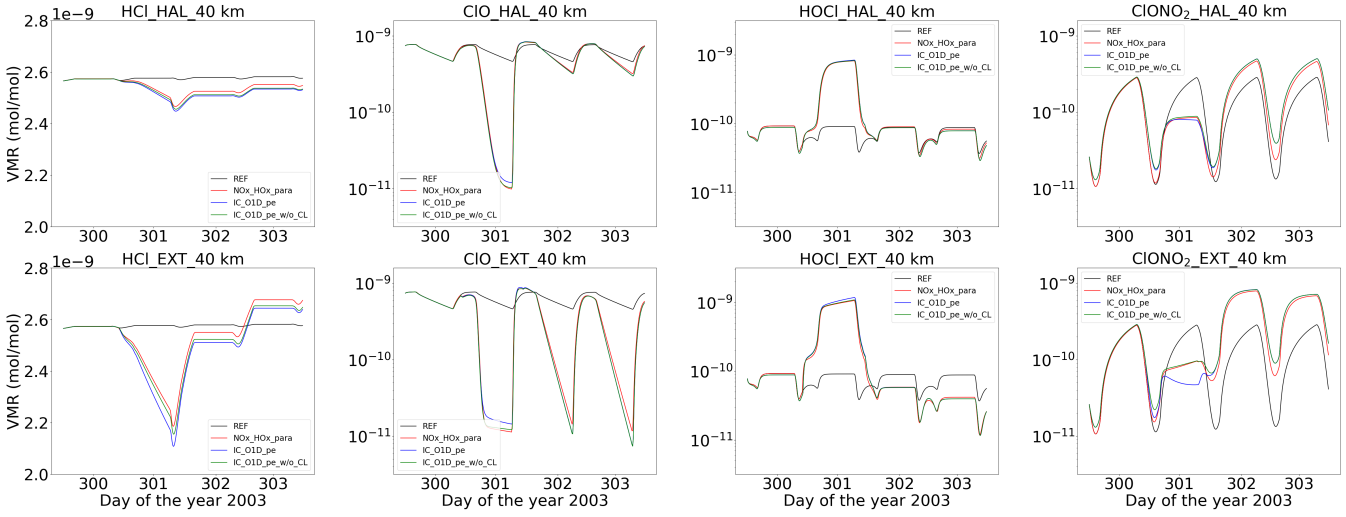

Figure 15. Comparison of the Halloween SPE and the extreme scenario for (column wise): HCl, ClO, HOCl and $ClONO_2$ at 40 km.

An interesting observation for HCl can be seen from the figure 15 for the extreme scenario, where the recovered HCl after the event shows a positive excursion. This depends on the diurnal cycle of ClO and happens mainly during night time. The reformation of HCl can happen via R11 and R12 during night time because during daytime HO_2 and H_2O_2 photolyses. This can be seen from the figure 16 where HO_2 and H_2O_2 production increases during the event mainly at night time. Since the chlorine atoms aren't enough during night time (also seen from the first plot of figure 16), a steep increase in HCl is observed during the transition from day to night, where Cl, HO_2 and H_2O_2 increases which is constant over the night and increases again afterwards at the beginning of the day.

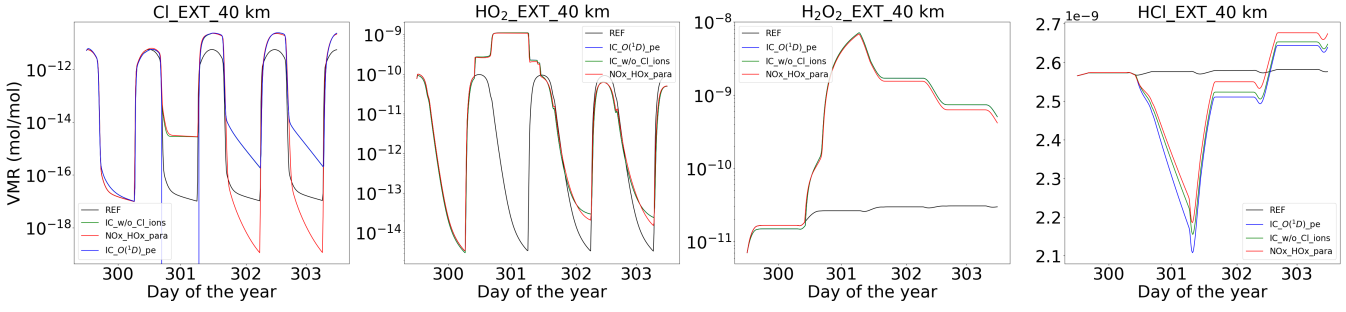

Figure 16. Volume mixing ratios of species (Cl, HO_2, H_2O_2 and HCl) at 40 km for the extreme event. The different lines are for the model settings: reference (black), ion-chemistry with $O(^1D)$ in photo-chemical equilibrium (blue), without chlorine ions (green) and parameterised NO_x and HO_x (red)

https://doi.org/10.5194/egusphere-2023-427
Preprint. Discussion started: 13 March 2023

4.3 Ozone:

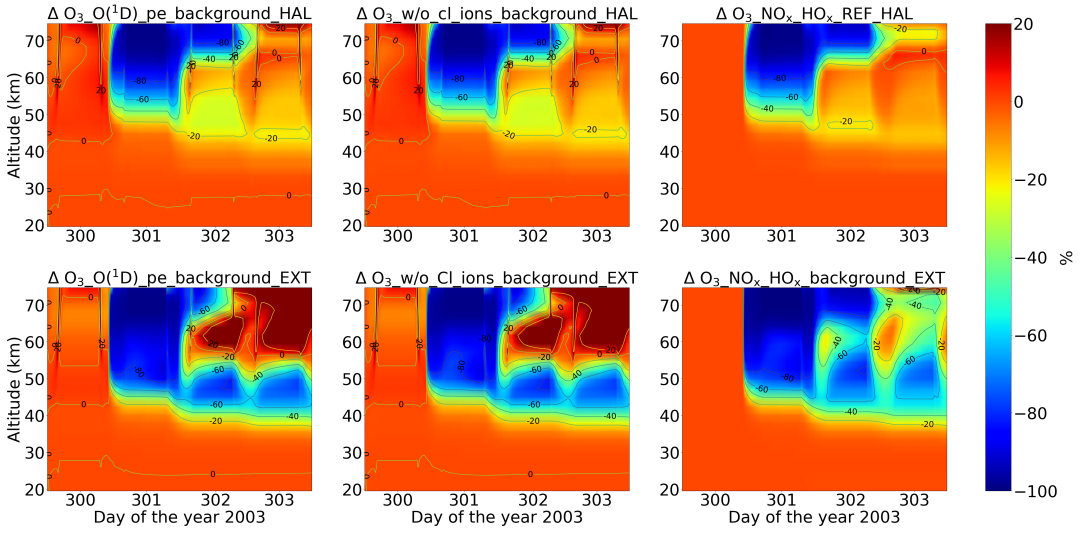

Figure 17. Percentage difference of ozone for the different model runs w.r.t. the reference run (row-wise): Halloween event and extreme scenario; (column-wise): ion-chemistry with O(^{1}D) in photochemical equilibrium, without Cl ions and parameterised NO_x and HO_x.

Figure 17 shows the percentage difference of ozone for the two events for the different model runs calculated w.r.t. the reference run. It is seen that with the onset of the event, ozone is completely lost, which is due to HO_x enhancements in the mesosphere above 55 km. This net ozone loss in the upper stratosphere and mesosphere is mainly due to odd hydrogen (HO_x) catalytic destruction cycles (R14 and R15) (Jackman et al., 2005) and is short-lived. Since HO_x species have a shorter lifetime, the recovery of ozone is faster. For the extreme event, after the event stops, ozone enhancements upto 25 % is observed in the mesosphere.

$N\tilde{O}_y$ is quite long lived down at 40 km altitude and below so the ozone loss due to the NO_x catalytic cycle seems to be persistent. The ozone loss occurs during day time when NO reacts with ozone to form NO_2, which is then photolysed back to NO and this catalytic cycle between NO and NO_2, related to daytime continues (see reactions R20 and R21). In the beginning, the amount of $N\tilde{O}_y$ was not enough for ozone loss but at the end of the event, the accumulation is large enough for significant ozone depletion which stays on and produces a diurnal cycle as seen from the Figure 17. The continuing ozone loss in the middle and upper stratosphere, after the event stops, is found to be still 80-100 % for the extreme scenario as compared to the Halloween event which is just around 20 %.

5 Impact of chlorine ions on ozone loss

The evaluation of the model results with MIPAS observations gave us confidence in the model. Thus, the impact of chlorine ion-chemistry on ozone loss could be assessed using the model. According to the model, we find the ozone loss in the stratosphere

https://doi.org/10.5194/egusphere-2023-427
Preprint. Discussion started: 13 March 2023

and lower mesosphere during the event. Figure 18 shows the relative difference of the ion-chemistry model with O(^{1}D) in photo-chemical equilibrium including chlorine ions w.r.t. the model without chlorine ions for daytime and night-time. The difference in this case here is calculated for daily averaged data for each day. A loss of 2.5 % during daytime at an altitude range of 40-60 km and about 10 % during night-time, at an altitude of 50-70 km is observed during the event day. Negative chlorine species directly increase the concentrations of uncharged active chlorine compounds. Through their catalytic cycles, these uncharged chlorine compounds through their catalytic cycles can be responsible for ozone loss at different altitudes which is also dependent on illumination conditions. The ClO_x catalytic cycle (R23 and R24) is responsible for the ozone loss at 40-50 km. There is a slight difference between day-time and night-time in the loss observed in terms of altitude range, which is expected. Loss of 0.6 % during day-time and 2 % during night-time is observed in the altitude range of 30-40 km, for which the ClO_x cycles with Reactions R31, R32, R33 and Reactions R35, R36, R37 and R38 are responsible. Furthermore, ozone formation of 2 % both during daytime and night-time around 60-70 km is observed after the event stops which is also due to the impact of chlorine ion-chemistry.

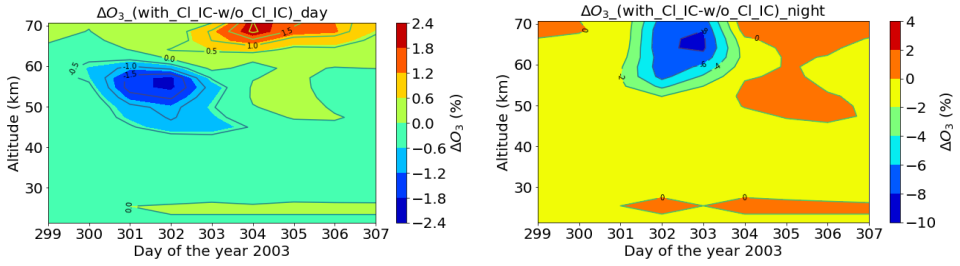

Figure 18. Relative difference of the model with full ion-chemistry and O(^{1}D) in photo-chemical equilibrium including chlorine ions w.r.t. the model without chlorine ion-chemistry for the Halloween SPE: daytime (left) and night-time (right). The difference here is calculated for daily averaged data.

Figure 19 shows the relative differences of the model setting with ion-chemistry and O(^{1}D) in photo-chemical equilibrium w.r.t. the model setting without chlorine ion-chemistry comparing the Halloween SPE and the extreme event in order to assess the impact of chlorine ion-chemistry on ozone loss during the event day. A very small impact of the chlorine ions around 10-20 % is observed on the event day. Qualitatively it was a bit more for the extreme event compared to the Halloween SPE, which could be more important for higher forcing. An increase of around 5 % for ozone is also seen after the event stops for the extreme scenario.

https://doi.org/10.5194/egusphere-2023-427
Preprint. Discussion started: 13 March 2023

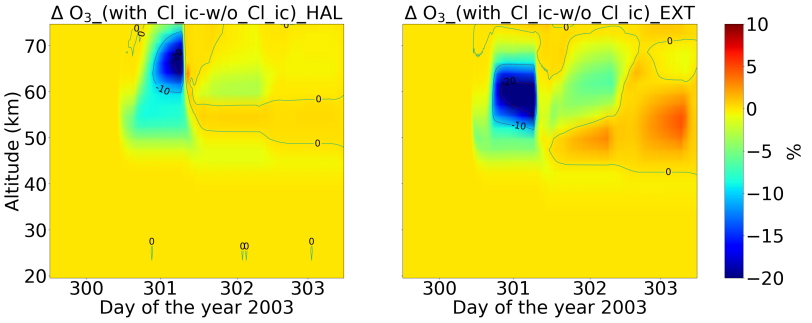

Figure 19. Relative difference of the model simulations: full ion-chemistry with O(^{1}D) in photo-chemical equilibrium and with chlorine ions w.r.t. the model setting without chlorine ion-chemistry comparing the Halloween SPE (left) and extreme scenario (right). The data shown here is not daily averaged but the real model time step.

6 Conclusions

Using satellite data (MIPAS on ENVISAT), the state of the art 1D ion-chemistry ExoTIC model has been validated. Two event classes were modelled and chlorine ion-chemistry and its impact on ozone has been evaluated. ExoTIC has been used to study the short-term constituent changes caused by the Halloween SPE of 2003. The results demonstrated here show a comparison of stratospheric and mesospheric composition changes observed by MIPAS in the polar cap region with simulations performed by ExoTIC. The inter-comparison of the model and MIPAS observations allowed for an evaluation of the overall ability of the ExoTIC model to reproduce observed atmospheric perturbations generated by solar proton events, particularly with respect to changes in the chlorine species, SPE induced NO_y enhancements and ozone depletion. Polar upper stratospheric and lower mesospheric NO_y increased by over 40 ppbv and mesospheric ozone decreased by over 70 % during the SPE period. The inter-comparison also tested and identified deficiencies in the chemical schemes, particularly with respect to nitrogen and chlorine chemistry which is relevant for stratospheric ozone. Short-time enhancements of HOCl and $ClONO_2$ were observed by MIPAS and also reproduced in the simulations with different model settings. Application of MIPAS averaging kernels to the ExoTIC output made the inter-comparison much better. HOCl enhancements were reproduced best for the model simulation with full ion-chemistry where O(^{1}D) was set to photo-chemical equilibrium. An HOCl enhancement of more than 0.2 ppbv occurred roughly during the event as observed by MIPAS. The HOCl enhancements with averaging kernels as found in ExoTIC and its temporal variation agree quite well with MIPAS. The ozone depletion simulated by the model extends over a large altitude range as compared to MIPAS observations. Jackman et al. (2008) found the opposite from WACCM3 results in the northern hemisphere in terms of altitude range. The encountered differences between the model and observations for $ClONO_2$ enhancements, it's underestimation by the model are related to a smaller availability of ClO in the polar region before the SPE. The $ClONO_2$ peak is observed at the same altitude for both the model and MIPAS, but the enhancements in MIPAS is observed earlier and the peak values seem to agree quite well even without the averaging kernels applied. Jackman et al. (2008) also

https://doi.org/10.5194/egusphere-2023-427
Preprint. Discussion started: 13 March 2023

found the $ClONO_2$ peak at the same altitude with WACCM3 but the values were underestimated by a factor of two compared to MIPAS.

The comparison of the Halloween SPE and the extreme solar event of 775 A.D. showed long lasting stratospheric ozone loss for the extreme scenario. A long lasting impact was also found for the chlorine species like HOCl and HCl in case of the extreme scenario. Loss of HCl was underestimated by the parameterised model which was also found by Winkler et al. (2009) during the solar proton event in July 2000 in the northern polar region. For the extreme event, the parameterised model showed a much higher NO_y enhancements, about a 1000 ppm in the mesosphere and lower thermosphere. HO_x enhancements of 0.1 ppm was found during the extreme event which went further down in altitude upto 40 km, for all the model case studies. An impact of around 10-20 % on ozone loss was found due to the chlorine ions for the two events, a bit stronger for the extreme scenario, which is more important for higher forcing. Ozone formation was observed after the event which is also due to the impact of chlorine ion-chemistry. For the Halloween event with temporal ionisation rates, ozone loss of 2.4 % during day-time and 10 % during night-time was observed during the event that is due to chlorine ion-chemistry. Ozone formation of 2-4 % was also found after the event both during day-time and night-time.

In general, ExoTIC simulations reproduced the impacts of the Halloween SPE quite well, mainly for HOCl and NO_y. However, the initial state of the atmosphere in the simulations could be an important factor for some variability in the model results and MIPAS observations. Future work will focus on including the D-region ion-chemistry into the global 3D chemistry climate model EMAC (ECHAM/MESSy) and the evaluation of the chemistry with MIPAS observations in a setup considering atmospheric dynamics.

https://doi.org/10.5194/egusphere-2023-427
Preprint. Discussion started: 13 March 2023

Appendix A: Chlorine Ions and Ionic Reactions

In this Appendix, the reactions involving the chlorine ions and their rate coefficients used in ExoTIC is listed.

Table A1. T is the temperature in K, and M is the total air density in cm^{-3}

Reactants	Products	Rate coefficient	Source
$Cl^- + Cl_2$	Cl_3^-	$9\times10^{-30}\times(M)$	Amelynck et al. (1994)
$Cl^- + CO_2$	$Cl^-(CO_2)$	$6\times10^{-29}\times(\frac{300}{T})^2\times(M)$	Kopp and Fritzenwallner (1997)
$Cl^- + H_2O$	$Cl^-(H_2O)$	$2\times10^{-29}\times(\frac{300}{T})^2\times(M)$	Turco (1977)
$Cl^- + HCl$	$Cl^-(HCl)$	$1\times10^{-27}\times(M)$	Kazil et al. (2003)
$Cl^-(CO_2)$	$Cl^- + CO_2$	$2.6\times10^{-5}\times(\frac{300}{T})^3\times e^{\frac{-4000}{T}}\times(M)$	Kopp and Fritzenwallner (1997)
$Cl^-(H_2O)$	$Cl^- + H_2O$	$9.2\times10^{-5}\times(\frac{300}{T})^3\times e^{\frac{-7450}{T}}\times(M)$	Kopp and Fritzenwallner (1997)
$Cl^-(HCl)$	$Cl^- + HCl$	$3.33\times10^{-5}\times(\frac{300}{T})\times e^{\frac{-11926}{T}}\times(M)$	Kopp and Fritzenwallner (1997)
$NO_3^- + HCl$	$NO_3^-(HCl)$	$5.22\times10^{-28}\times(\frac{300}{T})^{2.62}$	Kopp and Fritzenwallner (1997)
$OH^- + HCl$	$Cl^- + H_2O$	$1.5\times10^{-9}\times(\frac{300}{T})^5$	Kopp and Fritzenwallner (1997)
$Cl^- + ClONO_2$	$NO_3^- + Cl_2$	9.2×10^{-10}	Turco (1977)
$Cl^- + HNO_3$	$NO_3^- + HCl$	2.8×10^{-9}	Huey (1996)
$Cl^- + H$	$e + HCl$	9.6×10^{-10}	Turco (1977)
$Cl^- + N_2O_5$	$NO_3^- + ClNO_2$	9.4×10^{-10}	Amelynck et al. (1994)
$Cl^-(H_2O) + Cl_2$	$Cl_3^- + H_2$	1.09×10^{-9}	Kopp and Fritzenwallner (1997)
$Cl^-(H_2O) + HCl$	$Cl^-(HCl) + H_2O$	1.30×10^{-9}	Kopp and Fritzenwallner (1997)
$Cl^-(H_2O) + HNO_3$	$NO_3^-(HCl) + H_2O$	2.85×10^{-9}	Kopp and Fritzenwallner (1997)
$Cl^-(H_2O) + H$	$e + H_2O + HCl$	8×10^{-11}	Kopp and Fritzenwallner (1997)
$Cl^-(HCl) + Cl_2$	$Cl_3^- + HCl$	5.3×10^{-10}	Kopp and Fritzenwallner (1997)
$Cl^-(HCl) + HNO_3$	$NO_3^-(HCl) + HCl$	2.48×10^{9}	Kopp and Fritzenwallner (1997)
$Cl^- + NO_2$	$NO_2^- + Cl$	6.0×10^{-12}	Kopp and Fritzenwallner (1997)
$Cl^- + O_3$	$ClO^- + O_2$	5.0×10^{-13}	Turco (1977)
$Cl_2^- + HNO_3$	$NO_3^-(HCl) + Cl$	4.8×10^{-10}	Amelynck et al. (1994)
$Cl_2^- + NO_2$	$Cl^- + ClNO_2$	4.0×10^{-11}	Kopp and Fritzenwallner (1997)
$Cl_2^- + O_3$	$O_3^- + Cl_2$	2.0×10^{-12}	Kopp and Fritzenwallner (1997)
$Cl_3^- + HNO_3$	$NO_3^-(HCl) + Cl_2$	1.3×10^{-9}	Amelynck et al. (1994)
$CO_3^- + ClONO_2$	$NO_3^- + ClO + CO_2$	2.1×10^{-9}	Kopp and Fritzenwallner (1997)
$CO_3^- + HCl$	$Cl^- + OH + CO_2$	3.0×10^{-11}	Kopp and Fritzenwallner (1997)
$CO_4^- + HCl$	$Cl^-(HO_2) + CO_2$	1.2×10^{-11}	Kopp and Fritzenwallner (1997)

continued

https://doi.org/10.5194/egusphere-2023-427
Preprint. Discussion started: 13 March 2023

Reactants	Products	Rate coefficient	Source
$NO_2^- + Cl_2$	$Cl_2^- + NO_2$	6.8×10^{-10}	Kopp and Fritzenwallner (1997)
$NO_2^- + HCl$	$Cl^- + HNO_2$	1.4×10^{-9}	Kopp and Fritzenwallner (1997)
$NO_3^- + HCl$	$Cl^- + HNO_2$	1.0×10^{-12}	Kopp and Fritzenwallner (1997)
$NO_3^-(HCl) + HNO_3$	$NO_3^-(HNO_3) + HCl$	7.6×10^{-10}	Amelynck et al. (1994)
$O^- + HCl$	$Cl^- + OH$	2.0×10^{-9}	Turco (1977)
$O_2^- + HCl$	$Cl^- + HO_2$	1.6×10^{-9}	Turco (1977)
$O_3^- + Cl_2$	$Cl^- + ClO + O2$	1.3×10^{-9}	Turco (1977)
$ClO^- + NO$	$Cl^- + NO_2$	$2.9\times10^{-11}\times0.5$	Turco (1977)
$ClO^- + O_3$	$Cl^- + O_2 + O_2$	6.0×10^{-11}	Turco (1977)
$ClO^- + O_3$	$ClO + O_3^-$	1.0×10^{-11}	Turco (1977)
$O^- + Cl$	$Cl^- + O$	1.0×10^{-10}	Turco (1977)
$O^- + ClO$	$Cl^- + O_2$	1.0×10^{-10}	Turco (1977)
$O_2^- + Cl$	$Cl^- + O_2$	1.0×10^{-10}	Turco (1977)
$O_2^- + ClO$	$ClO^- + O_2$	1.0×10^{-10}	Turco (1977)
$OH^- + Cl$	$Cl^- + OH$	1.0×10^{-10}	Turco (1977)
$OH^- + ClO$	$ClO^- + OH$	1.0×10^{-10}	Turco (1977)
$CO_3^- + Cl$	$Cl^- + O + CO_2$	1.0×10^{-10}	Turco (1977)
$CO_3^- + Cl$	$ClO^- + CO_2$	1.0×10^{-10}	Turco (1977)
$CO_3^- + ClO$	$Cl^- + CO_2 + O_2$	1.0×10^{-10}	Turco (1977)
$CO_4^- + Cl$	$Cl^- + O_2 + CO_2$	1.0×10^{-10}	Turco (1977)
$CO_4^- + ClO$	$ClO^- + O_2 + CO_2$	1.0×10^{-10}	Turco (1977)
$NO_2^- + Cl$	$Cl^- + NO_2$	1.0×10^{-10}	Turco (1977)
$NO_2^- + ClO$	$Cl^- + NO_3$	1.0×10^{-10}	Turco (1977)
$HCO_3^- + Cl$	$Cl^- + OH + CO_2$	1.0×10^{-10}	Turco (1977)
$HCO_3^- + ClO$	$Cl^- + HO_2 + CO_2$	1.0×10^{-10}	Turco (1977)
$ClO^- + O$	$Cl^- + O_2$	2.0×10^{-10}	Turco (1977)
$H^+ + Cl^-$	Cl	$6\times10^{-8}\times(\frac{300}{T})^{0.5}+1.25\times10^{-25}\times(\frac{300}{T})^{4}\times(M)^*$	Arijs et al. (1987)
$H^+ + Cl_2^-$	Cl_2		
$H^+ + Cl_3^-$	$Cl_2 + Cl$		
$H^+ + Cl^-(HCl)$	$Cl + HCl$		
$H^+ + Cl^-(H_2O)$	$Cl + H_2O$		

* The coefficient is the same for all the reactions below

https://doi.org/10.5194/egusphere-2023-427
Preprint. Discussion started: 13 March 2023

Reactants	Products	Rate coefficient	Source
$H^+ + Cl^-(CO_2)$	$Cl + CO_2$		
$H^+ + Cl^-(HO_2)$	$Cl + HO_2$		
$H^+ + ClO^-$	ClO		

Code availability. The Exoplanetary Terrestrial Ion Chemistry (EXoTIC) is continuously developed and applied in the group 'Middle Atmosphere Solar Variability and Climate Interactions (MSK)' at IMK-ASF. The exact code version used to produce the simulation results can be made available upon request from Miriam Sinnhuber (miriam.sinnhuber@kit.edu).

Data availability. MIPAS data are available from https://www.imk-asf.kit.edu/english/308.php (Institute of Meteorology and Climate Research, 2022) after registration.

Author contributions. MB and MS discussed the ideas. MB wrote the paper. MB and MS worked on the code and simulation results for the ExoTIC ion-chemistry model. MB worked on the visualisation and analysis the MIPAS data and AL helped with the MIPAS averaging kernels. TC, GS and BF provided access to MIPAS data and helped with technical questions regarding the correct use of MIPAS data. JW and OY developed AISstorm and provided us with the ionisation rates. IU calculated the ionisation rates for the extreme solar event of 775 A.D. All authors contributed to reviewing and editing the manuscript.

Competing interests. At least one of the co-authors is a member of the editorial board of Atmospheric Chemistry and Physics.

Acknowledgements. This research has been supported by the German Research Foundation (DFG) under the project SI 1088/7-1.

https://doi.org/10.5194/egusphere-2023-427
Preprint. Discussion started: 13 March 2023

References

Amelynck, C., Fussen, D., and Arijs, E.: Reactions of nitric acid with di- and trichloride ions, di- and tri-iodide ions and with CO-4 in the gas phase, International Journal of Mass Spectrometry and Ion Processes, 133, 13–28, https://doi.org/https://doi.org/10.1016/0168-1176(94)03950-X, 1994.

Arijs, E., Nevejans, D., and Ingels, J.: Stratospheric positive ion composition measurements and acetonitrile detection: a consistent picture?, International Journal of Mass Spectrometry and Ion Processes, 81, 15–31, https://doi.org/https://doi.org/10.1016/0168-1176(87)80003-4, 1987.

Barth, C. A.: Nitric oxide in the lower thermosphere, Planetary and Space Science, 40, 315–336, https://doi.org/https://doi.org/10.1016/0032-0633(92)90067-X, 1992.

Bates, D. R. and Nicolet, M.: The photochemistry of atmospheric water vapor, Journal of Geophysical Research (1896-1977), 55, 301–327, https://doi.org/https://doi.org/10.1029/JZ055i003p00301, 1950.

Chakrabarty, D. and Ganguly, S.: On significant quantities of negative ions observed around the mesopause, Journal of Atmospheric and Terrestrial Physics, 51, 983–989, https://doi.org/https://doi.org/10.1016/0021-9169(89)90013-5, 1989.

Chipperfield, M. P.: Multiannual simulations with a three-dimensional chemical transport model, Journal of Geophysical Research: Atmospheres, 104, 1781–1805, https://doi.org/https://doi.org/10.1029/98JD02597, 1999.

Connor, B. J., Siskind, D. E., Tsou, J. J., Parrish, A., and Remsberg, E. E.: Ground-based microwave observations of ozone in the upper stratosphere and mesosphere, , 99, 16,757–16,770, https://doi.org/10.1029/94JD01153, 1994.

Damiani, A., Funke, B., Marsh, D. R., López-Puertas, M., Santee, M. L., Froidevaux, L., Wang, S., Jackman, C. H., von Clarmann, T., Gardini, A., Cordero, R. R., and Storini, M.: Impact of January 2005 solar proton events on chlorine species, Atmospheric Chemistry and Physics, 12, 4159–4179, https://doi.org/10.5194/acp-12-4159-2012, 2012.

Daniel, J. S., Solomon, S., Portmann, R. W., and Garcia, R. R.: Stratospheric ozone destruction: The importance of bromine relative to chlorine, Journal of Geophysical Research: Atmospheres, 104, 23 871–23 880, https://doi.org/https://doi.org/10.1029/1999JD900381, 1999.

Fischer, H., Birk, M., Blom, C., Carli, B., Carlotti, M., von Clarmann, T., Delbouille, L., Dudhia, A., Ehhalt, D., Endemann, M., Flaud, J. M., Gessner, R., Kleinert, A., Koopman, R., Langen, J., López-Puertas, M., Mosner, P., Nett, H., Oelhaf, H., Perron, G., Remedios, J., Ridolfi, M., Stiller, G., and Zander, R.: MIPAS: an instrument for atmospheric and climate research, Atmospheric Chemistry and Physics, 8, 2151–2188, https://doi.org/10.5194/acp-8-2151-2008, 2008.

Fritzenwallner, J. and Kopp, E.: Model calculations of the negative ion chemistry in the mesosphere with special emphasis on the chlorine species and the formation of cluster ions, Advances in Space Research, 21, 891–894, https://doi.org/https://doi.org/10.1016/S0273-1177(97)00649-2, proceedings of the C0.1 Symposium of COSPAR Scientific Commission C, 1998.

Funke, B., López-Puertas, M., Gil-López, S., von Clarmann, T., Stiller, G. P., Fischer, H., and Kellmann, S.: Downward transport of upper atmospheric NOx into the polar stratosphere and lower mesosphere during the Antarctic 2003 and Arctic 2002/2003 winters, Journal of Geophysical Research: Atmospheres, 110, https://doi.org/https://doi.org/10.1029/2005JD006463, 2005a.

Funke, B., López-Puertas, M., von Clarmann, T., Stiller, G. P., Fischer, H., Glatthor, N., Grabowski, U., Höpfner, M., Kellmann, S., Kiefer, M., Linden, A., Mengistu Tsidu, G., Milz, M., Steck, T., and Wang, D. Y.: Retrieval of stratospheric NOx from 5.3 and 6.2 μm nonlocal thermodynamic equilibrium emissions measured by Michelson Interferometer for Passive Atmospheric Sounding (MIPAS) on Envisat, Journal of Geophysical Research: Atmospheres, 110, https://doi.org/https://doi.org/10.1029/2004JD005225, 2005b.

https://doi.org/10.5194/egusphere-2023-427
Preprint. Discussion started: 13 March 2023

Funke, B., Baumgaertner, A., Calisto, M., Egorova, T., Jackman, C. H., Kieser, J., Krivolutsky, A., López-Puertas, M., Marsh, D. R., Reddmann, T., Rozanov, E., Salmi, S.-M., Sinnhuber, M., Stiller, G. P., Verronen, P. T., Versick, S., von Clarmann, T., Vyushkova, T. Y., Wieters, N., and Wissing, J. M.: Composition changes after the "Halloween" solar proton event: the High Energy Particle Precipitation in the Atmosphere (HEPPA) model versus MIPAS data intercomparison study, Atmospheric Chemistry and Physics, 11, 9089–9139, https://doi.org/10.5194/acp-11-9089-2011, 2011.

Glatthor, N., von Clarmann, T., Fischer, H., Funke, B., Gil-López, S., Grabowski, U., Höpfner, M., Kellmann, S., Linden, A., López-Puertas, M., Mengistu Tsidu, G., Milz, M., Steck, T., Stiller, G. P., and Wang, D.-Y.: Retrieval of stratospheric ozone profiles from MIPAS/ENVISAT limb emission spectra: a sensitivity study, Atmospheric Chemistry and Physics, 6, 2767–2781, https://doi.org/10.5194/acp-6-2767-2006, 2006.

Harvey, V. L., Randall, C. E., and Collins, R. L.: Chemical definition of the mesospheric polar vortex, Journal of Geophysical Research: Atmospheres, 120, 10,166–10,179, https://doi.org/https://doi.org/10.1002/2015JD023488, 2015.

Herbst, K., Grenfell, J. L., Sinnhuber, M., and Wunderlich, F.: INCREASE: An updated model suite to study the INfluence of Cosmic Rays on Exoplanetary AtmoSpherEs, Astronomische Nachrichten, 343, e210 072, https://doi.org/https://doi.org/10.1002/asna.20210072, 2022.

Höpfner, M., von Clarmann, T., Fischer, H., Funke, B., Glatthor, N., Grabowski, U., Kellmann, S., Kiefer, M., Linden, A., Milz, M., Steck, T., Stiller, G. P., Bernath, P., Blom, C. E., Blumenstock, T., Boone, C., Chance, K., Coffey, M. T., Friedl-Vallon, F., Griffith, D., Hannigan, J. W., Hase, F., Jones, N., Jucks, K. W., Keim, C., Kleinert, A., Kouker, W., Liu, G. Y., Mahieu, E., Mellqvist, J., Mikuteit, S., Notholt, J., Oelhaf, H., Piesch, C., Reddmann, T., Ruhnke, R., Schneider, M., Strandberg, A., Toon, G., Walker, K. A., Warneke, T., Wetzel, G., Wood, S., and Zander, R.: Validation of MIPAS $ClONO_2$ measurements, Atmospheric Chemistry and Physics, 7, 257–281, https://doi.org/10.5194/acp-7-257-2007, 2007.

Huey, L.: The kinetics of the reactions of Cl-, O-, and O2- with HNO3: Implications for measurement of HNO3 in the atmosphere, International Journal of Mass Spectrometry and Ion Processes, 153, 145–150, https://doi.org/https://doi.org/10.1016/0168-1176(95)04354-3, 1996.

J. C. Farman, B. G. G. and Shanklin., J. D.: Large losses of total ozone in Antarctica reveal seasonal ClOx/NOx interaction, Nature, 315, 207–210, https://doi.org/10.1038/315207a0, 1985.

Jackman, C. H., Fleming, E. L., and Vitt, F. M.: Influence of extremely large solar proton events in a changing stratosphere, Journal of Geophysical Research: Atmospheres, 105, 11 659–11 670, https://doi.org/https://doi.org/10.1029/2000JD900010, 2000.

Jackman, C. H., DeLand, M. T., Labow, G. J., Fleming, E. L., Weisenstein, D. K., Ko, M. K., Sinnhuber, M., and Russell, J. M.: Neutral atmospheric influences of the solar proton events in October–November 2003, Journal of Geophysical Research: Space Physics, 110, 2005.

Jackman, C. H., Marsh, D. R., Vitt, F. M., Garcia, R. R., Fleming, E. L., Labow, G. J., Randall, C. E., López-Puertas, M., Funke, B., von Clarmann, T., and Stiller, G. P.: Short- and medium-term atmospheric constituent effects of very large solar proton events, Atmospheric Chemistry and Physics, 8, 765–785, https://doi.org/10.5194/acp-8-765-2008, 2008.

Jones, R. and Rees, M.: Time dependent studies of the aurora—I. Ion density and composition, Planetary and Space Science, 21, 537–557, https://doi.org/https://doi.org/10.1016/0032-0633(73)90069-X, 1973.

Kazil, J., Kopp, E., Chabrillat, S., and Bishop, J.: The University of Bern Atmospheric Ion Model: Time-dependent modeling of the ions in the mesosphere and lower thermosphere, Journal of Geophysical Research: Atmospheres, 108, https://doi.org/https://doi.org/10.1029/2002JD003024, 2003.

https://doi.org/10.5194/egusphere-2023-427
Preprint. Discussion started: 13 March 2023

Kopp, E. and Fritzenwallner, J.: Chlorine and bromine ions in the D-region, Advances in Space Research, 20, 2111–2115, https://doi.org/https://doi.org/10.1016/S0273-1177(97)00603-0, middle Atmosphere: Changes and Electrodynamics, 1997.

Kvissel, O.-K., Orsolini, Y. J., Stordal, F., Isaksen, I. S. A., and Santee, M. L.: Formation of stratospheric nitric acid by a hydrated ion cluster reaction: Implications for the effect of energetic particle precipitation on the middle atmosphere, Journal of Geophysical Research: Atmospheres, 117, https://doi.org/https://doi.org/10.1029/2011JD017257, 2012.

Lary, D. J.: Catalytic destruction of stratospheric ozone, Journal of Geophysical Research: Atmospheres, 102, 21 515–21 526, https://doi.org/https://doi.org/10.1029/97JD00912, 1997.

López-Puertas, M., Funke, B., Gil-López, S., von Clarmann, T., Stiller, G. P., Höpfner, M., Kellmann, S., Fischer, H., and Jackman, C. H.: Observation of NOx enhancement and ozone depletion in the Northern and Southern Hemispheres after the October–November 2003 solar proton events, Journal of Geophysical Research: Space Physics, 110, https://doi.org/https://doi.org/10.1029/2005JA011050, 2005.

Mekhaldi, F., Muscheler, R., Adolphi, F., Aldahan, A., Beer, J., Mcconnell, J., Possnert, G., Sigl, M., Svensson, A., Synal, H.-A., Welten, K., and Woodruff, T.: Multiradionuclide evidence for the solar origin of the cosmic-ray events of AD 774/5 and 993/4, Nature communications, 6, 8611, https://doi.org/10.1038/ncomms9611, 2015.

Meyer, P., Parker, E. N., and Simpson, J. A.: Solar Cosmic Rays of February, 1956 and Their Propagation through Interplanetary Space, Phys. Rev., 104, 768–783, https://doi.org/10.1103/PhysRev.104.768, 1956.

Nieder, H., Winkler, H., Marsh, D., and Sinnhuber, M.: NOx production due to energetic particle precipitation in the MLT region: Results from ion chemistry model studies, 119, 2014.

Porter, H. S., Jackman, C. H., and Green, A. E. S.: Efficiencies for production of atomic nitrogen and oxygen by relativistic proton impact in air, The Journal of Chemical Physics, 65, 154–167, https://doi.org/10.1063/1.432812, 1976.

Rusch, D., Gérard, J.-C., Solomon, S., Crutzen, P., and Reid, G.: The effect of particle precipitation events on the neutral and ion chemistry of the middle atmosphere—I. Odd nitrogen, Planetary and Space Science, 29, 767–774, https://doi.org/https://doi.org/10.1016/0032-0633(81)90048-9, 1981.

Sander, S., Golden, D., Kurylo, M., Moortgat, G., Wine, P., Ravishankara, A., Kolb, C., Molina, M., Finlayson-Pitts, B., Huie, R., et al.: Chemical kinetics and photochemical data for use in atmospheric studies evaluation number 15, Tech. rep., Pasadena, CA: Jet Propulsion Laboratory, National Aeronautics and Space . . . , 2006.

Sinnhuber, M., Nieder, H., and Wieters, N.: Energetic Particle Precipitation and the Chemistry of the Mesosphere/Lower Thermosphere, Surveys in Geophysics, 33, https://doi.org/10.1007/s10712-012-9201-3, 2012.

Solomon, S., Rusch, D., Gérard, J., Reid, G., and Crutzen, P.: The effect of particle precipitation events on the neutral and ion chemistry of the middle atmosphere: II. Odd hydrogen, Planetary and Space Science, 29, 885–893, https://doi.org/https://doi.org/10.1016/0032-0633(81)90078-7, 1981.

Stiller, G. P., Kiefer, M., Eckert, E., von Clarmann, T., Kellmann, S., García-Comas, M., Funke, B., Leblanc, T., Fetzer, E., Froidevaux, L., Gomez, M., Hall, E., Hurst, D., Jordan, A., Kämpfer, N., Lambert, A., McDermid, I. S., McGee, T., Miloshevich, L., Nedoluha, G., Read, W., Schneider, M., Schwartz, M., Straub, C., Toon, G., Twigg, L. W., Walker, K., and Whiteman, D. N.: Validation of MIPAS IMK/IAA temperature, water vapor, and ozone profiles with MOHAVE-2009 campaign measurements, Atmospheric Measurement Techniques, 5, 289–320, https://doi.org/10.5194/amt-5-289-2012, 2012.

Sukhodolov, T., Usoskin, I. G., Rozanov, E. V., Asvestari, E., Ball, W. T., Curran, M. A. J., Fischer, H., Kovaltsov, G. A., Miyake, F., Peter, T., Plummer, C., Schmutz, W. K., Severi, M., and Traversi, R.: Atmospheric impacts of the strongest known solar particle storm of 775 AD, Scientific Reports, 7, 2017.

https://doi.org/10.5194/egusphere-2023-427
Preprint. Discussion started: 13 March 2023

Swider, W. and Keneshea, T.: Decrease of ozone and atomic oxygen in the lower mesosphere during a PCA event, Planetary and Space Science, 21, 1969–1973, https://doi.org/https://doi.org/10.1016/0032-0633(73)90126-8, 1973.

Turco, R. P.: On the formation and destruction of chlorine negative ions in the D region, Journal of Geophysical Research (1896-1977), 82, 3585–3592, https://doi.org/https://doi.org/10.1029/JA082i025p03585, 1977.

Usoskin, I. G. and Kovaltsov, G. A.: OCCURRENCE OF EXTREME SOLAR PARTICLE EVENTS: ASSESSMENT FROM HISTORICAL PROXY DATA, The Astrophysical Journal, 757, 92, https://doi.org/10.1088/0004-637x/757/1/92, 2012.

Usoskin, I. G., Kromer, B., Ludlow, F., Beer, J., Friedrich, M., Kovaltsov, G. A., Solanki, S. K., and Wacker, L.: The AD775 cosmic event revisited: the Sun is to blame, Astronomy and Astrophysics, 552, 2013.

Verronen, P. T., Andersson, M. E., Marsh, D. R., Kovács, T., and Plane, J. M. C.: WACCM-D—Whole Atmosphere Community Climate Model with D-region ion chemistry, Journal of Advances in Modeling Earth Systems, 8, 954–975, https://doi.org/https://doi.org/10.1002/2015MS000592, 2016.

von Clarmann, T., Glatthor, N., Höpfner, M., Kellmann, S., Ruhnke, R., Stiller, G. P., Fischer, H., Funke, B., Gil-López, S., and López-Puertas, M.: Experimental evidence of perturbed odd hydrogen and chlorine chemistry after the October 2003 solar proton events, Journal of Geophysical Research: Space Physics, 110, https://doi.org/https://doi.org/10.1029/2005JA011053, 2005.

von Clarmann, T., Glatthor, N., Grabowski, U., Höpfner, M., Kellmann, S., Linden, A., Mengistu Tsidu, G., Milz, M., Steck, T., Stiller, G. P., Fischer, H., and Funke, B.: Global stratospheric HOCl distributions retrieved from infrared limb emission spectra recorded by the Michelson Interferometer for Passive Atmospheric Sounding (MIPAS), Journal of Geophysical Research: Atmospheres, 111, https://doi.org/https://doi.org/10.1029/2005JD005939, 2006.

von Clarmann, T., Funke, B., Glatthor, N., Kellmann, S., Kiefer, M., Kirner, O., Sinnhuber, B.-M., and Stiller, G. P.: The MIPAS HOCl climatology, Atmospheric Chemistry and Physics, 12, 1965–1977, https://doi.org/10.5194/acp-12-1965-2012, 2012.

von Clarmann, T., Degenstein, D. A., Livesey, N. J., Bender, S., Braverman, A., Butz, A., Compernolle, S., Damadeo, R., Dueck, S., Eriksson, P., Funke, B., Johnson, M. C., Kasai, Y., Keppens, A., Kleinert, A., Kramarova, N. A., Laeng, A., Langerock, B., Payne, V. H., Rozanov, A., Sato, T. O., Schneider, M., Sheese, P., Sofieva, V., Stiller, G. P., von Savigny, C., and Zawada, D.: Overview: Estimating and reporting uncertainties in remotely sensed atmospheric composition and temperature, Atmospheric Measurement Techniques, 13, 4393–4436, https://doi.org/10.5194/amt-13-4393-2020, 2020.

Weeks, L. H., Cuikay, R. S., and Corbin, J. R.: Ozone Measurements in the Mesosphere During The Solar Proton Event of 2 November 1969, Journal of Atmospheric Sciences, 29, 1138 – 1142, https://doi.org/10.1175/1520-0469(1972)029<1138:OMITMD>2.0.CO;2, 1972.

Winkler, H., Kazeminejad, S., Sinnhuber, M., Kallenrode, M.-B., and Notholt, J.: Conversion of mesospheric HCl into active chlorine during the solar proton event in July 2000 in the northern polar region, Journal of Geophysical Research: Atmospheres, 114, https://doi.org/https://doi.org/10.1029/2008JD011587, 2009.

Wissing, J. M. and Kallenrode, M.-B.: Atmospheric Ionization Module Osnabrück (AIMOS): A 3-D model to determine atmospheric ionization by energetic charged particles from different populations, Journal of Geophysical Research: Space Physics, 114, https://doi.org/https://doi.org/10.1029/2008JA013884, 2009.